2024-2025

THÈSE

pour le

DIPLÔME D'ÉTAT DE DOCTEUR EN MÉDECINE

Qualification en Radiologie

Retrograde interpretation of chest X-rays by reproducing radiological signs from CT images using the "direct volume rendering" technique

Interprétation rétrograde de radiographies thoraciques en reproduisant les signes radiologiques à partir d'images CT grâce à la technique de « rendu volumique direct »

GRANGEREAU Aurore

Née le 28/12/1997 à Soissons (02)

Sous la direction de Dr. ABI KHALIL Samer

Membres du jury

Pr WILLOTEAUX Serge	Président
Dr ABI KHALIL Samer	Directeur
Dr GOURDIER Anne Laurence	Membre
Dr DROUET Claire	Membre

Soutenue publiquement le :
21/08/2025

FACULTÉ DE SANTÉ
UNIVERSITÉ D'ANGERS

ENGAGEMENT DE NON PLAGIAT

Je, soussignée GRANGEREAU Aurore
déclare être pleinement consciente que le plagiat de documents ou d'une partie d'un document publiée sur toutes formes de support, y compris l'internet, constitue une violation des droits d'auteur ainsi qu'une fraude caractérisée.
En conséquence, je m'engage à citer toutes les sources que j'ai utilisées pour écrire ce rapport ou mémoire.

signé par l'étudiante le **09/06/2024**

SERMENT D'HIPPOCRATE

« Au moment d'être admise à exercer la médecine, je promets et je jure d'être fidèle aux lois de l'honneur et de la probité. Mon premier souci sera de rétablir, de préserver ou de promouvoir la santé dans tous ses éléments, physiques et mentaux, individuels et sociaux. Je respecterai toutes les personnes, leur autonomie et leur volonté, sans aucune discrimination selon leur état ou leurs convictions. J'interviendrai pour les protéger si elles sont affaiblies, vulnérables ou menacées dans leur intégrité ou leur dignité. Même sous la contrainte, je ne ferai pas usage de mes connaissances contre les lois de l'humanité. J'informerai les patients des décisions envisagées, de leurs raisons et de leurs conséquences. Je ne tromperai jamais leur confiance et n'exploiterai pas le pouvoir hérité des circonstances pour forcer les consciences. Je donnerai mes soins à l'indigent et à quiconque me les demandera. Je ne me laisserai pas influencer par la soif du gain ou la recherche de la gloire.

Admise dans l'intimité des personnes, je tairai les secrets qui me seront confiés. Reçue à l'intérieur des maisons, je respecterai les secrets des foyers et ma conduite ne servira pas à corrompre les mœurs. Je ferai tout pour soulager les souffrances. Je ne prolongerai pas abusivement les agonies. Je ne provoquerai jamais la mort délibérément.

Je préserverai l'indépendance nécessaire à l'accomplissement de ma mission. Je n'entreprendrai rien qui dépasse mes compétences. Je les entretiendrai et les perfectionnerai pour assurer au mieux les services qui me seront demandés.

J'apporterai mon aide à mes confrères ainsi qu'à leurs familles dans l'adversité. Que les hommes et mes confrères m'accordent leur estime si je suis fidèle à mes promesses ; que je sois déshonorée et méprisée si j'y manque ».

LISTE DES ENSEIGNANTS DE LA FACULTÉ DE SANTÉ D'ANGERS

Doyen de la Faculté : Pr Cédric ANNWEILER
Vice-Doyen de la Faculté et directeur du département de pharmacie : Pr Sébastien FAURE
Directeur du département de médecine : Pr Vincent DUBEE

PROFESSEURS DES UNIVERSITÉS

ABRAHAM Pierre	PHYSIOLOGIE	Médecine
ANGOULVANT Cécile	MEDECINE GENERALE	Médecine
ANNWEILER Cédric	GERIATRIE ET BIOLOGIE DU VIEILLISSEMENT	Médecine
ASFAR Pierre	REANIMATION	Médecine
AUBE Christophe	RADIOLOGIE ET IMAGERIE MEDICALE	Médecine
AUGUSTO Jean-François	NEPHROLOGIE	Médecine
BAUFRETON Christophe	CHIRURGIE THORACIQUE ET CARDIOVASCULAIRE	Médecine
BELLANGER William	MEDECINE GENERALE	Médecine
BELONCLE François	REANIMATION	Médecine
BIERE Loïc	CARDIOLOGIE	Médecine
BIGOT Pierre	UROLOGIE	Médecine
BONNEAU Dominique	GENETIQUE	Médecine
BOUCHARA Jean-Philippe	PARASITOLOGIE ET MYCOLOGIE	Médecine
BOUET Pierre-Emmanuel	GYNECOLOGIE-OBSTETRIQUE	Médecine
BOURSIER Jérôme	GASTROENTEROLOGIE ; HEPATOLOGIE	Médecine
BOUVARD Béatrice	RHUMATOLOGIE	Médecine
BRIET Marie	PHARMACOLOGIE	Médecine
CAMPONE Mario	CANCEROLOGIE ; RADIOTHERAPIE	Médecine
CAROLI-BOSC François-Xavier	GASTROENTEROLOGIE ; HEPATOLOGIE	Médecine
CASSEREAU Julien	NEUROLOGIE	Médecine
CLERE Nicolas	PHARMACOLOGIE / PHYSIOLOGIE	Pharmacie
COLIN Estelle	GENETIQUE	Médecine
CONNAN Laurent	MEDECINE GENERALE	Médecine
COPIN Marie-Christine	ANATOMIE ET CYTOLOGIE PATHOLOGIQUES	Médecine
COUTANT Régis	PEDIATRIE	Médecine
CUSTAUD Marc-Antoine	PHYSIOLOGIE	Médecine
CRAUSTE-MANCIET Sylvie	PHARMACOTECHNIE HOSPITALIERE	Pharmacie
DE CASABIANCA Catherine	MEDECINE GENERALE	Médecine
DERBRE Séverine	PHARMACOGNOSIE	Pharmacie
DESCAMPS Philippe	GYNECOLOGIE-OBSTETRIQUE	Médecine
D'ESCATHA Alexis	MEDECINE ET SANTE AU TRAVAIL	Médecine
DINOMAIS Mickaël	MEDECINE PHYSIQUE ET DE READAPTATION	Médecine

DUBEE Vincent	MALADIES INFECTIEUSES ET TROPICALES	Médecine
DUCANCELLE Alexandra	BACTERIOLOGIE-VIROLOGIE ; HYGIENE HOSPITALIERE	Médecine
DUVERGER Philippe	PEDOPSYCHIATRIE	Médecine
EVEILLARD Matthieu	BACTERIOLOGIE-VIROLOGIE	Pharmacie
FAURE Sébastien	PHARMACOLOGIE PHYSIOLOGIE	Pharmacie
FOURNIER Henri-Dominique	ANATOMIE	Médecine
FOUQUET Olivier	CHIRURGIE THORACIQUE ET CARDIOVASCULAIRE	Médecine
FURBER Alain	CARDIOLOGIE	Médecine
GAGNADOUX Frédéric	PNEUMOLOGIE	Médecine
GOHIER Bénédicte	PSYCHIATRIE D'ADULTES	Médecine
GUARDIOLA Philippe	HEMATOLOGIE ; TRANSFUSION	Médecine
GUILET David	CHIMIE ANALYTIQUE	Pharmacie
HUNAULT-BERGER Mathilde	HEMATOLOGIE ; TRANSFUSION	Médecine
JEANNIN Pascale	IMMUNOLOGIE	Médecine
KAZOUR François	PSYCHIATRIE	Médecine
KEMPF Marie	BACTERIOLOGIE-VIROLOGIE ; HYGIENE HOSPITALIERE	Médecine
KUN-DARBOIS Daniel	CHIRURGIE MAXILLO-FACIALE ET STOMATOLOGIE	Médecine
LACOEUILLE FRANCK	RADIOPHARMACIE	Pharmacie
LACCOURREYE Laurent	OTO-RHINO-LARYNGOLOGIE	Médecine
LAGARCE Frédéric	BIOPHARMACIE	Pharmacie
LANDREAU Anne	BOTANIQUE/ MYCOLOGIE	Pharmacie
LASOCKI Sigismond	ANESTHESIOLOGIE-REANIMATION	Médecine
LEBDAI Souhil	UROLOGIE	Médecine
LEGENDRE Guillaume	GYNECOLOGIE-OBSTETRIQUE	Médecine
LEGRAND Erick	RHUMATOLOGIE	Médecine
LEMEE Jean-Michel	NEUROCHIRURGIE	Médecine
LERMITE Emilie	CHIRURGIE GENERALE	Médecine
LEROLLE Nicolas	REANIMATION	Médecine
LIBOUBAN Hélène	HISTOLOGIE	Médecine
LUQUE PAZ Damien	HEMATOLOGIE BIOLOGIQUE	Médecine
MARCHAIS Véronique	BACTERIOLOGIE-VIROLOGIE	Pharmacie
MARTIN Ludovic	DERMATO-VENEREOLOGIE	Médecine
MAY-PANLOUP Pascale	BIOLOGIE ET MEDECINE DU DEVELOPPEMENT ET DE LA REPRODUCTION	Médecine
MENEI Philippe	NEUROCHIRURGIE	Médecine
MERCAT Alain	REANIMATION	Médecine
ORVAIN Corentin	HEMATOLOGIE ; TRANSFUSION	Médecine
PAISANT Anita	RADIOLOGIE	Médecine
PAPON Nicolas	PARASITOLOGIE ET MYCOLOGIE MEDICALE	Pharmacie
PASSIRANI Catherine	CHIMIE GENERALE	Pharmacie
PELLIER Isabelle	PEDIATRIE	Médecine

PETIT Audrey	MEDECINE ET SANTE AU TRAVAIL	Médecine
PICQUET Jean	CHIRURGIE VASCULAIRE ; MEDECINE VASCULAIRE	Médecine
PODEVIN Guillaume	CHIRURGIE INFANTILE	Médecine
PROCACCIO Vincent	GENETIQUE	Médecine
PRUNIER Delphine	BIOCHIMIE ET BIOLOGIE MOLECULAIRE	Médecine
PRUNIER Fabrice	CARDIOLOGIE	Médecine
PY Thibaut	MEDECINE GENERALE	Médecine
RAMOND-ROQUIN Aline	MEDECINE GENERALE	Médecine
REYNIER Pascal	BIOCHIMIE ET BIOLOGIE MOLECULAIRE	Médecine
RIOU Jérémie	BIOSTATISTIQUE	Pharmacie
RINEAU Emmanuel	ANESTHESIOLOGIE REANIMATION	Médecine
RIQUIN Elise	PEDOPSYCHIATRIE ; ADDICTOLOGIE	Médecine
RODIEN Patrice	ENDOCRINOLOGIE, DIABETE ET MALADIES METABOLIQUES	Médecine
ROQUELAURE Yves	MEDECINE ET SANTE AU TRAVAIL	Médecine
ROUGE-MAILLART Clotilde	MEDECINE LEGALE ET DROIT DE LA SANTE	Médecine
ROUSSEAU Audrey	ANATOMIE ET CYTOLOGIE PATHOLOGIQUES	Médecine
ROUSSEAU Pascal	CHIRURGIE PLASTIQUE, RECONSTRUCTRICE ET ESTHETIQUE	Médecine
ROUSSELET Marie-Christine	ANATOMIE ET CYTOLOGIE PATHOLOGIQUES	Médecine
ROY Pierre-Marie	MEDECINE D'URGENCE	Médecine
SAULNIER Patrick	BIOPHYSIQUE ET BIOSTATISTIQUES	Pharmacie
SERAPHIN Denis	CHIMIE ORGANIQUE	Pharmacie
SCHMIDT Aline	HEMATOLOGIE ; TRANSFUSION	Médecine
TESSIER-CAZENEUVE Christine	MEDECINE GENERALE	Médecine
TRZEPIZUR Wojciech	PNEUMOLOGIE	Médecine
UGO Valérie	HEMATOLOGIE ; TRANSFUSION	Médecine
URBAN Thierry	PNEUMOLOGIE	Médecine
VAN BOGAERT Patrick	PEDIATRIE	Médecine
VENARA Aurélien	CHIRURGIE VISCERALE ET DIGESTIVE	Médecine
VENIER-JULIENNE Marie-Claire	PHARMACOTECHNIE	Pharmacie
VERNY Christophe	NEUROLOGIE	Médecine
WILLOTEAUX Serge	RADIOLOGIE ET IMAGERIE MEDICALE	Médecine

MAÎTRES DE CONFÉRENCES

AMMI Myriam	CHIRURGIE VASCULAIRE ET THORACIQUE	Médecine
BAGLIN Isabelle	CHIMIE THERAPEUTIQUE	Pharmacie
BASTIAT Guillaume	BIOPHYSIQUE ET BIOSTATISTIQUES	Pharmacie
BEAUVILLAIN Céline	IMMUNOLOGIE	Médecine

BEGUE Cyril	MEDECINE GENERALE	Médecine
BELIZNA Cristina	MEDECINE INTERNE	Médecine
BENOIT Jacqueline	PHARMACOLOGIE	Pharmacie
BERNARD Florian	ANATOMIE	Médecine
BESSAGUET Flavien	PHYSIOLOGIE PHARMACOLOGIE	Pharmacie
BLANCHET Odile	HEMATOLOGIE ; TRANSFUSION	Médecine
BOISARD Séverine	CHIMIE ANALYTIQUE	Pharmacie
BOUCHER Sophie	ORL	Médecine
BRIET Claire	ENDOCRINOLOGIE, DIABETE ET MALADIES METABOLIQUES	Médecine
BRILLAND Benoit	NEPHROLOGIE	Médecine
BRIS Céline	BIOCHIMIE ET BIOLOGIE MOLECULAIRE	Pharmacie
BRUGUIERE Antoine	PHARMACOGNOSIE	Pharmacie
CAPITAIN Olivier	CANCEROLOGIE ; RADIOTHERAPIE	Médecine
CHABRUN Floris	BIOCHIMIE ET BIOLOGIE MOLECULAIRE	Pharmacie
CHAO DE LA BARCA Juan-Manuel	BIOCHIMIE ET BIOLOGIE MOLECULAIRE	Médecine
CHOPIN Matthieu	MEDEECINE GENERALE	
CODRON Philippe	NEUROLOGIE	Médecine
DEMAS Josselin	SCIENCES DE LA READAPTATION	Médecine
DESHAYES Caroline	BACTERIOLOGIE VIROLOGIE	Pharmacie
DOUILLET Delphine	MEDECINE D'URGENCE	Médecine
FERRE Marc	BIOLOGIE MOLECULAIRE	Médecine
FORTRAT Jacques-Olivier	PHYSIOLOGIE	Médecine
GHALI Maria	MEDECINE GENERALE	Médecine
GUELFF Jessica	MEDECINE GENERALE	Médecine
HADJ MAHMOUD Dorra	IMMUNOLOGIE	Pharma
HAMEL Jean-François	BIOSTATISTIQUES, INFORMATIQUE MEDICALE	Médicale
HAMON Cédric	MEDECINE GENERALE	Médecine
HELESBEUX Jean-Jacques	CHIMIE ORGANIQUE	Pharmacie
HERIVAUX Anaïs	BIOTECHNOLOGIE	Pharmacie
HINDRE François	BIOPHYSIQUE	Médecine
JOUSSET-THULLIER Nathalie	MEDECINE LEGALE ET DROIT DE LA SANTE	Médecine
JUDALET-ILLAND Ghislaine	MEDECINE GENERALE	Médecine
KHIATI Salim	BIOCHIMIE ET BIOLOGIE MOLECULAIRE	Médecine
LEFEUVRE Caroline	BACTERIOLOGIE ; VIROLOGIE	Médecine
LEGEAY Samuel	PHARMACOCINETIQUE	Pharmacie
LEPELTIER Elise	CHIMIE GENERALE	Pharmacie
LETOURNEL Franck	BIOLOGIE CELLULAIRE	Médecine
MABILLEAU Guillaume	HISTOLOGIE, EMBRYOLOGIE ET CYTOGENETIQUE	Médecine
MALLET Sabine	CHIMIE ANALYTIQUE	Pharmacie
MAROT Agnès	PARASITOLOGIE ET MYCOLOGIE MEDICALE	Pharmacie
MESLIER Nicole	PHYSIOLOGIE	Médecine
MIOT Charline	IMMUNOLOGIE	Médecine
MOUILLIE Jean-Marc	PHILOSOPHIE	Médecine
NAIL BILLAUD Sandrine	IMMUNOLOGIE	Pharmacie

PAILHORIES Hélène	BACTERIOLOGIE-VIROLOGIE	Médecine
PAPON Xavier	ANATOMIE	Médecine
PASCO-PAPON Anne	RADIOLOGIE ET IMAGERIE MEDICALE	Médecine
PENCHAUD Anne-Laurence	SOCIOLOGIE	Médecine
PIHET Marc	PARASITOLOGIE ET MYCOLOGIE	Médecine
PIRAUX Arthur	OFFICINE	Pharmacie
POIROUX Laurent	SCIENCES INFIRMIERES	Médecine
RONY Louis	CHIRURGIE ORTHOPEDIQUE ET TRAUMATOLOGIQUE	Médecine
ROGER Emilie	PHARMACOTECHNIE	Pharmacie
SAVARY Camille	PHARMACOLOGIE-TOXICOLOGIE	Pharmacie
SCHMITT Françoise	CHIRURGIE INFANTILE	Médecine
SCHINKOWITZ Andréas	PHARMACOGNOSIE	Pharmacie
SPIESSER-ROBELET Laurence	PHARMACIE CLINIQUE ET EDUCATION THERAPEUTIQUE	Pharmacie
TEXIER-LEGENDRE Gaëlle	MEDECINE GENERALE	Médecine
VIAULT Guillaume	CHIMIE ORGANIQUE	Pharmacie

AUTRES ENSEIGNANTS

ATER		
BARAKAT Fatima	CHIMIE ANALYTIQUE	Pharmacie
ATCHADE Constantin	GALENIQUE	Pharmacie
PRCE		
AUTRET Erwan	ANGLAIS	Santé
BARBEROUSSE Michel	INFORMATIQUE	Santé
COYNE Ashley	ANGLAIS	Santé
O'SULLIVAN Kayleigh	ANGLAIS	Santé
RIVEAU Hélène	ANGLAIS	
PAST-MAST		
AUBRUCHET Hélène		
BEAUVAIS Vincent	OFFICINE	Pharmacie
BRAUD Cathie	OFFICINE	Pharmacie
CAVAILLON Pascal	PHARMACIE INDUSTRIELLE	Pharmacie
DILÉ Nathalie	OFFICINE	Pharmacie
GUILLET Anne-Françoise	PHARMACIE DEUST PREPARATEUR	Pharmacie
MOAL Frédéric	PHARMACIE CLINIQUE	Pharmacie
CHAMPAGNE Romain	MEECINE PHYSIQUE ET READAPTATION	Médecine
KAASSIS Mehdi	GASTRO-ENTEROLOGIE	Médecine
GUITTON Christophe	MEDECINE INTENSIVE-REANIMATION	Médecine
LAVIGNE Christian	MEDECINE INTERNE	Médecine
PICCOLI Giorgina	NEPHROLOGIE	Médecine
POMMIER Pascal	CANCEROLOGIE-RADIOTHERAPIE	Médecine
SAVARY Dominique	MEDECINE D'URGENCE	Médecine
PLP		
CHIKH Yamina	ECONOMIE-GESTION	Médecine

REMERCIEMENTS

Au Dr. Abi Khalil, mon directeur de thèse,
Je voudrais te remercier sincèrement de m'avoir proposé ce travail de thèse, que j'ai trouvé passionnant du début à la fin. Tu as su me soutenir et me rassurer dans les moments de doute, en gardant toujours confiance dans la faisabilité et l'aboutissement de ce travail. Ton regard bienveillant, ta disponibilité et ton écoute ont été d'un grand réconfort tout au long de ce parcours. Je suis aussi particulièrement touchée que tu aies cru en mes dessins pour illustrer cette thèse. Le fait d'avoir pu y apporter cette part plus personnelle, a vraiment compté pour moi. Enfin, je tiens à te remercier pour ton aide précieuse et tout ce que tu m'as transmis durant mes stages et mes gardes à tes côtés – j'en garderai un souvenir marquant et formateur !

Au Pr. Willoteaux,
Je vous remercie infiniment pour l'honneur que vous me faites en présidant ce jury. Je suis reconnaissante du temps et de l'intérêt que vous avez consacré à la lecture et à l'évaluation de mon travail de thèse. Votre aide et la bienveillance dont vous avez fait preuve à mon égard durant mes périodes de stage en radio C ont beaucoup compté pour moi, en particulier dans les moments où je me sentais un peu (voire complètement) dépassée et perdue face aux scanners cardiaques…

Au Dr. Gourdier,
Merci de m'avoir fait l'honneur d'accepter de faire partie de mon jury de thèse et d'avoir pris le temps de lire ce travail avec soin et considération. Je te remercie également pour ton accompagnement attentif et chaleureux durant les stages, et pour la qualité de tes conseils tout au long de cette période. J'espère qu'un jour, grâce à ton enseignement, les pneumopathies interstitielles n'auront plus aucun secret pour moi !

Au Dr. Drouet,
Merci beaucoup d'avoir accepté de faire partie de mon jury de thèse. Ton enthousiasme pour le sujet de ma thèse m'a profondément touchée et m'a donné envie de me surpasser dans la réalisation de ce projet. J'espère avoir tenu mon pari, et que ce manuscrit aura pu t'apporter quelques éléments utiles pour ta pratique.

A mes chefs d'Angers et du Mans,
Je tiens à vous remercier sincèrement pour votre patience, votre disponibilité et votre accompagnement tout au long de ces années. Votre bienveillance, vos conseils et la qualité de votre enseignement ont profondément marqué ma formation. Je n'oublierai pas ce que vous m'avez transmis, ni la gentillesse avec laquelle vous l'avez fait.

REMERCIEMENTS

A maman,
Merci pour ton amour inconditionnel et ton soutien constant. Je n'aurais pas pu espérer meilleure maman. Mon enfance a été si belle à tes côtés, remplie de douceur et de sécurité. En grandissant, notre lien a évolué : tu es devenue ma confidente et ma meilleure amie. Très tôt, tu m'as transmis le goût de la médecine et tu m'as toujours donné les moyens de poursuivre mes rêves. Tu as su me donner la force d'avancer et de me dépasser. Je ne te remercierai jamais assez pour tout cela. Je t'aime.

A papa,
Merci de m'avoir autant aimée et soutenu pendant toutes ces années. Ta tendresse, ta force tranquille et ton amour inconditionnel ont été si rassurants pour la petite fille que j'étais et pour la femme que je suis devenue. Merci pour l'indéfectible confiance que tu as en moi, qui m'a permis de gagner en assurance. Je veux que tu saches que je suis extrêmement fière d'être ta fille. Je n'en serai certainement pas là aujourd'hui sans ton aide. Alors merci infiniment, je t'aime.

A Maxime,
J'ai eu de la chance de grandir avec toi (même si tu ne m'as jamais laissée gagner aux jeux vidéo). Avec les années, tu es resté le même : toujours là, à m'écouter avec attention et bienveillance. Je suis si fière de la personne que tu es devenue, un père aimant et attentif. Te voir t'épanouir dans ce rôle avec tant de générosité et de douceur est une grande source de joie et d'admiration pour moi.

A Thomas,
Merci pour notre enfance où tu passais ton temps à faire le clown juste pour nous faire rire. Je n'oublie pas non plus ton soutien précieux pendant le concours de la P1, à un moment où je doutais vraiment de moi et où j'étais prête à abandonner, merci beaucoup.

A Agathe,
Merci infiniment d'avoir été ma relectrice officielle sur cette thèse ! On ne se connait pas depuis tant d'années mais tu occupes déjà une importante place dans ma vie (oui, je sais, tu vas trouver ça niais, mais quand c'est vrai, il faut savoir le dire !). J'adore nos discussions et nos partages de potins qui peuvent durer des heures, nos échanges de vidéos de chat sans parler de nos week-ends à bouffer. Alors là, c'est carrément le graal !

A Julien G.,
Merci à toi pour ces soirées endiablées à danser à tes côtés (même si je ne me fais aucune illusion sur le fait que tu me surpasses et que ça ne va pas aller en s'arrangeant), que j'apprécie autant que nos petits moments plus tranquilles à papoter de tout et rien. Ta bonne humeur et ta joie de vivre sont un exemple pour moi.

A Clémence,
Tu es ma plus ancienne amie, celle avec qui j'ai traversé la « magnifique » période de l'adolescence (bon dieu, qu'on était belles avec nos franges rideaux !) et à qui j'ai toujours tout pu dire. Tu comptes énormément pour moi, et même si on se voit moins souvent qu'avant, rien ne change entre nous. Chaque fois qu'on se retrouve, c'est comme si rien n'avait changé.
Je sais que ta vie n'est pas facile en ce moment mais saches que je ne t'oublie pas et que je serai toujours là si tu as besoin de moi.

A Antoinette,
Merci à toi pour ta bienveillance et ta douceur constante. Tu es l'une de mes plus belles rencontres au Mans et même si une petite distance nous sépare désormais, j'espère te revoir aussi souvent que possible. Je te souhaite le meilleur du monde, tu ne mérites rien de moins.

REMERCIEMENTS

A mes amis du Mansque (je pourrai vous énumérez mais vous êtes nombreux, vous saurez vous reconnaitre de toute manière), avec mention spéciale pour **le comité (Dorine, Alix, Benoit, Marie, Camille, Charly, Claire-Hélo et Emma V.)** :
Merci du fond du cœur pour tous ces moments incroyables que l'on a partagés : les fous rires, les bons repas, les soirées endiablées… autant de souvenirs qui resteront gravés dans ma mémoire. Et merci aussi pour tout ce qu'on continue à vivre aujourd'hui — en particulier nos discussions qui partent dans tous les sens, et que j'adore toujours autant.
Vous avez embelli mon internat bien au-delà de ce que j'aurais pu imaginer, et j'espère que vous serez là aussi pour illuminer les prochaines étapes de ma vie.

A mes co-internes (Lyronn, Sylvain, Blandine, Alix, Julien A., David, Naïma, Walid, Thomas, Zoé, Matthieu, Malala, Lucas, Marine…et tous ceux que j'ai oublié de citer ici avec lesquels j'ai moins eu le temps de travailler sans parler de ceux qui ont upgradé entre temps (coucou Jocelyn)),
Merci à vous avec qui j'ai eu la chance de partager ces années d'internat. J'ai adoré découvrir et apprendre notre beau métier à vos côtés. Vous avez su rendre les vacations plus légères, les midis plus sereins et chaque pause bien plus drôle. J'espère sincèrement que nos chemins continueront à se croiser, au travail comme ailleurs.

A Julien N., bon mec, t'es officiellement dans les remerciements de cette thèse, alors fais un effort… et fais pas ton radin pour les cadeaux ! Ahah. Blague à part (mais pas tant en vrai), merci pour ta bonne humeur contagieuse et ton humour caustique qui me fait rire malgré moi — même si j'en suis pas toujours très fière. Et surtout, merci d'être toujours là pour Aub's, ça vaut de l'or !

A Emeline, je suis tellement heureuse que tu aies été ma première rencontre à Angers. Arriver dans une ville où je ne connaissais personne n'était pas évident, mais te rencontrer a tout de suite rendu les choses plus simples et rassurantes. J'adore nos soirées papote et encore plus maintenant avec la petite Vroum en guest-star !

À Emma F., dommage qu'on ne soit plus voisines, c'était quand même bien sympa cette époque ! Et puis là, on ne s'est pas juste éloignées d'un quartier…il a fallu que tu partes en Nouvelle-Calédonie, rien que ça ! T'as bien raison de profiter de la vie, mais reviens vite nous voir quand même — tu nous manques.

A ma belle-famille,
Merci de m'avoir accueillie avec tant de gentillesse et de générosité. J'ai beaucoup de chance d'avoir rejoint une famille comme la vôtre. Nous avons déjà partagé de très beaux moments, et j'espère qu'il y en aura encore beaucoup d'autres à venir.

Et enfin pour finir en beauté, **à mon amour, ma branche,**
Je tiens à te remercier tout particulièrement pour ton soutien indéfectible tout au long de cette thèse. Tu as été là du début à la fin, toujours présent, toujours attentionné — et en plus, tu m'as régalée de bons petits plats (je suis vraiment vernie !). Ta relecture attentive, patiente (et franchement courageuse) de mon manuscrit m'a beaucoup rassurée. À charge de revanche, bien sûr…
Au-delà de cette thèse, je ne te remercierai jamais assez d'être entré dans ma vie. Tu es devenu mon pilier au quotidien, celui sur qui je peux toujours compter. Merci d'être là dans les bons comme les moins bons moments, de me supporter même quand je pars en vrille, et de me faire rire comme toi seul sais le faire. J'ai hâte de faire plein de projets avec toi, je t'aime.

List of abbreviations

CXT	Chest radiography
CT	Computed tomography
MPVR	Multiplanar volumic reformation
PACS	Picture archiving and communication system
SVC	Duplicated left superior vena cava
SAT	Supra-aortic trunks

Plan

RETROGRADE INTERPRETATION OF CHEST X-RAYS BY REPRODUCING RADIOLOGICAL SIGNS FROM CT IMAGES USING THE « DIRECT VOLUME RENDERING » TECHNIQUE.

GRANGEREAU Aurore[1;] ABI KHALIL Samer[2]

1 : Radiology Department, Angers University Hospital, Angers, France.

2 : Univ Angers, Inserm, CNRS, MITOVASC, Equipe CarMe ou Equipe MitoLab, SFR ICAT, F-49000 Angers, France. Radiology Department, Angers University Hospital, Angers, France.

ABSTRACT

Retrograde interpretation of chest X-rays by reproducing radiological signs from CT images using the "direct volume rendering" technique

Introduction

The standard chest X-ray remains the foundational tool in thoracic imaging. However, its proper interpretation is not always straightforward and requires a thorough understanding of the radiologic signs responsible for the observed radiographic appearances. This knowledge is essential for building an appropriate differential diagnosis and guiding further imaging with CT.

Objectives

- To highlight and identify semiological signs on chest X-ray through MPVR (Multiplanar Volume Rendering) reconstructions from CT images.
- To learn how to retrospectively reconstruct the macroscopic appearance of thoracic lesions on chest X-ray based on increasingly overlooked radiological signs.

Take-Home Message

There are four main categories of anatomical regions or structures that are prone to misinterpretation on chest radiography:

1) Anatomical Variants of the mediastinal structures and radiological illusions

Anatomical variants, especially congenital anomalies with no clinical expression, are frequent sources of confusion. These include azygos arch prominence due to azygos continuation of the inferior vena cava, right-sided aortic arch, bronchogenic and pleuropericardial cysts. A precise knowledge of normal anatomical appearances and their variations—nowadays often forgotten due to the predominance of CT—is essential.

2) Perception of mediastinal lesions

The mediastinum contains multiple anatomical interfaces oriented in different planes, making their boundaries challenging to interpret. Abnormalities involving paratracheal and paravertebral lines are frequently misread. Reliable interpretation requires an understanding of how mediastinal anatomical structures reflect onto the chest X-ray, producing characteristic two-dimensional interface signs.

3) Blind spots or hidden areas

There are pitfall zones in chest X-ray interpretation due to increased opacity related to normal anatomical structures. These include the lung apices, hilar regions, retrocardiac area, and the regions beneath the diaphragmatic domes.

4) Identification of key signs for the localization of thoracic opacities

Several signs help determine the exact location of a thoracic opacity and confirm its pulmonary origin. These include the silhouette sign, cervicothoracic sign, thoracoabdominal sign, and the contour angle between the opacity and adjacent thoracic wall. These signs allow for the reconstruction of the opacity's macroscopic appearance and for determining its anatomical relationships within the thorax.

INTRODUCTION

Chest radiography (CXR) remains the most commonly prescribed (1) and readily accessible imaging modality for the screening, diagnosis, and follow-up of thoracic pathologies. A thorough interpretation of the chest X-ray is essential for every medical student, resident, and practicing physician. This requires a solid initial understanding of the normal appearance of a chest X-ray. With a mental representation of a normal CXR, one can assess the quality of the image obtained, identify anatomical variants and diagnostic pitfalls, and, of course, detect potential lesions.

There are two main types of bias that account for most errors in chest X-ray interpretation: perceptual error and cognitive error (2). Perceptual error refers to the failure to visualize an abnormality on a radiograph even though it is present (3). This type of bias accounts for 60 to 80% of all radiologic errors (4-5) and explains the high number of missed diagnoses (3). Cognitive error, on the other hand, occurs when the abnormality is correctly detected on the radiograph but is misinterpreted in terms of its nature and clinical implications. The prevalence of radiologist errors has been estimated at 4% in practice, in which a substantial percentage of the cases are in fact normal (5, 6). The false-positive rate is 2% (6). However, the incidence of errors may be as high as 30% when the cases show abnormalities (6-8). This further reflects the challenges of accurate detection of CXR abnormalities, even among experienced observers.

On the other hand, three fundamental principles in chest X-ray interpretation contribute to a high-quality analysis: search and detection, recognition, and decision (9). The key elements for performing a high-quality chest radiograph analysis consist of a thorough

visual assessment of the various thoracic components. This process notably relies on the identification of multiple overlapping lines and stripes superimposed on a two-dimensional (2D) plane by a translation of complex three-dimensional (3D) structures. These lines and stripes are created by the interfaces between the lung parenchyma, the pleura, and the mediastinum (10). A solid understanding of their normal appearance and how they are altered in the setting of disease is an essential prerequisite for detecting potential pathology and narrowing down the differential diagnosis—even before obtaining additional information from a chest CT scan (10). Moreover, the failure to recognize an abnormality on a chest radiograph may lead to the omission of necessary additional investigations and potentially result in a delayed diagnosis.

In this study, we employed a CT-based tool known as Multi-Planar Volume Reformation (MPVR) to enhance the detection of radiological signs that healthcare professionals should be aware of. MPVR is an old but inventive tool that can reproduce from a chest CT scan a CXR substitute focused on an anatomic region that can help perceive anatomic relationships and discern subtle signs (11). This study allowed a more accurate retrospective interpretation of CXR with improved distinction of thoracic structures and detection of signs, using MPVR as a teaching tool.

MATERIALS AND METHODS

Imaging studies of adult patients were compiled by a radiology resident as part of this project. The compilation included frontal chest X-rays and chest CT scans of patients over 18 years old with predefined thoracic pathologies, in which an abnormality was already visible on the chest X-ray. Posteroanterior radiographs of acceptable quality were preferentially selected. All imaging studies available since the implementation of the PACS were considered potentially eligible. Relevant cases were identified by searching the PACS database of Angers University Hospital using keywords related to the targeted pathologies.

For each selected CT scan, the resident adjusted the MPVR reconstruction slice thickness to optimally highlight the radiographic signs of interest. A comparative analysis was then performed between each CT scan and its corresponding chest X-ray to emphasize key diagnostic features. This process enhanced the retrospective accuracy of chest X-ray interpretation.

The English translation and overall improvement of linguistic clarity in this manuscript were assisted by the use of the ChatGPT language model (OpenAI).

PICTORIAL REVIEW

On a properly positioned frontal CXR, there are four main factors to be assessed for overlooked lesions and signs, especially in difficult areas:

1 - Recognition of anatomical variants and radiological illusions

2 - Detection of mediastinal lesions

3 - Discernment of blind spots or hidden areas

4 - Identification of key signs for the localization of thoracic opacities

1. Anatomical variants of the mediastinal structures and radiological illusions

Due to their asymptomatic or nonspecific presentation, anatomical variants are typically discovered as incidental findings on CXR or CT scans. These anatomical variants may occur in isolation or in association with other anomalies as part of syndromic presentations. It is not uncommon for such variants to go unnoticed, particularly due to the lack of thorough visual analysis of thoracic anatomical structures — especially since chest X-rays are often initially ordered to investigate intrapulmonary lesions. The following section illustrates the imaging features of the main anatomical variations and congenital anomalies of the thoracic cage and mediastinum.

1.1. Thoracic cage variants

Medical personnel must be familiar with common anatomical variations of the thoracic cage and their radiographic appearance. A leftward deviation of the cardiac silhouette is typically observed in cases of ipsilateral volume loss (such as atelectasis) or contralateral lung hyperinflation (as in pneumothorax). However, this appearance can also be seen in the context of pectus excavatum (fig. 1) (12-13).

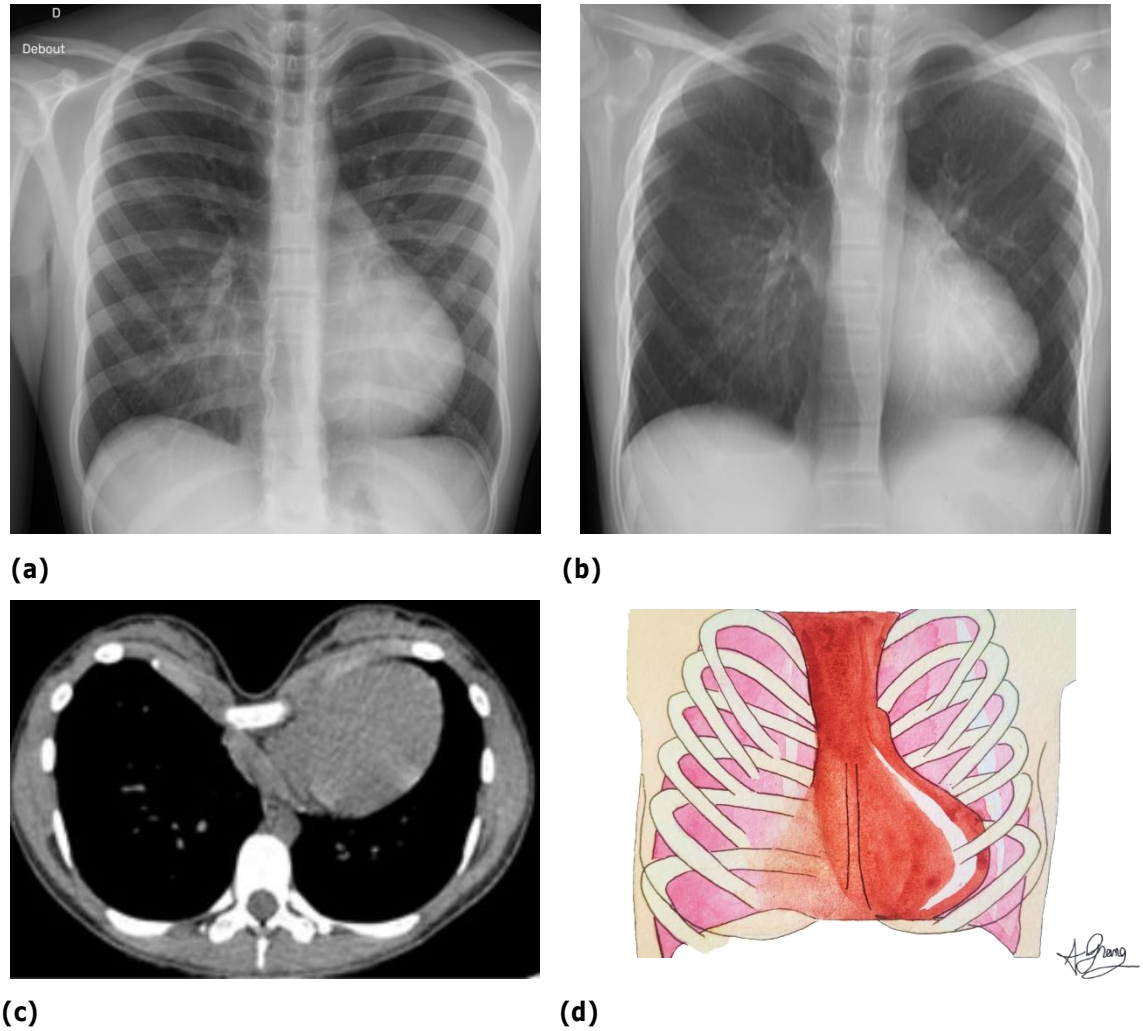

Fig. 1. Pectus excavatum: Frontal chest X-ray **(a)** and coronal CT scan with MPVR reformatting (slice thickness: 128 mm) in lung window **(b)** characteristically demonstrate a blurred right heart border, with a leftward displacement of the heart and increased opacity in the inferomedial region of the right lung (13-14). At the level of the ribs, there is a horizontal alignment of the posterior rib arches and vertical orientation of the anterior arches, resulting in a characteristic « heart-shaped appearance ». Axial CT scan in mediastinal window **(c)** clearly shows the concave deformity of the sternum. Diagram **(d)** illustrates a pectus excavatum.

Rib lesions may mimic pulmonary pathology (14). An incidental nodule may in fact correspond to costochondral calcification or to consolidation of a costal callus (fig. 2).

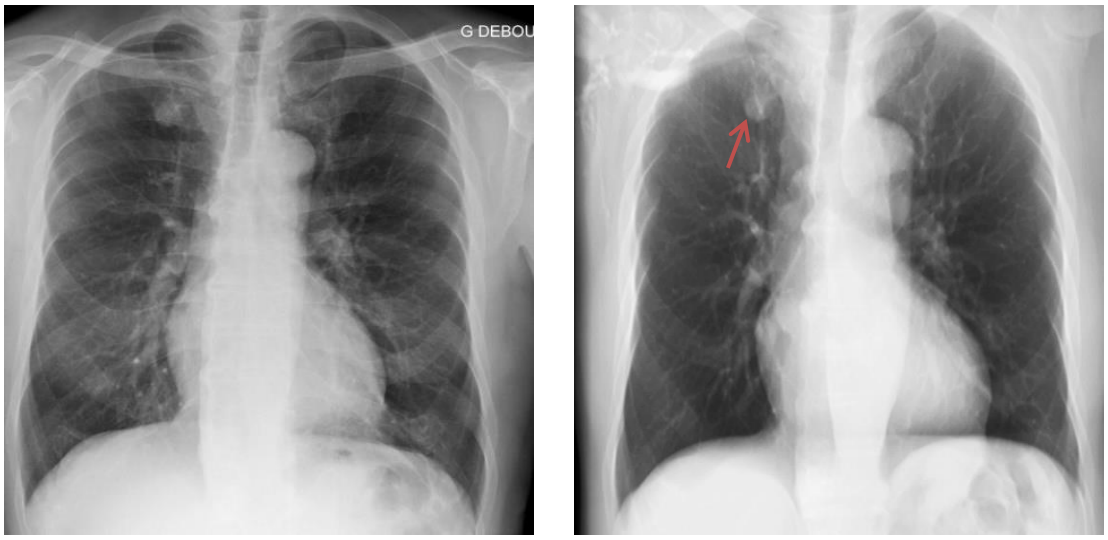

(a) **(b)**

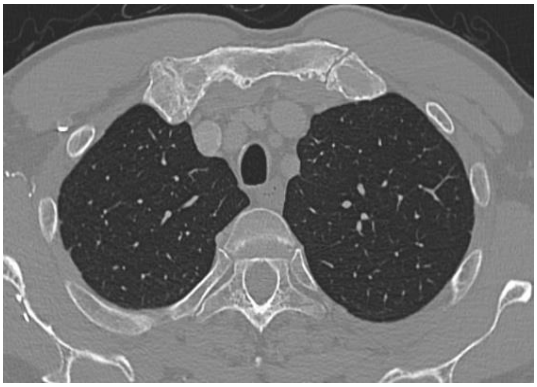

(c)

Fig. 2. Centimetric pseudonodule (red arrow) in the right upper lobe on frontal chest X-ray **(a)**. Coronal CT scan with MPVR reformatting (slice thickness: 128 mm) in lung window **(b)** and axial CT scan in bone window **(c)** show calcification of costochondral cartilage of the right first rib. This, combined with the medial border of the first rib simulates a pulmonary nodule. Within this pseudonodular image, lines corresponding to the edges of the rib and the calcified chostochondral cartilage can be distinguished.

Most of the time, chest radiography is sufficient to differentiate a normal rib variant from a true pathological process. In more challenging cases, a CT scan may be necessary to distinguish a true rib lesion from a pulmonary nodule (14).

1.2. Dextrocardia

Dextrocardia refers to the right-sided position of the heart, without necessarily implying a reversal of the position of the patient's other organs. This means that dextrocardia can occur in isolation, with the modal anatomical position of the other organs retained, or as part of a situs inversus with inversion of the position of other organs (fig. 3).

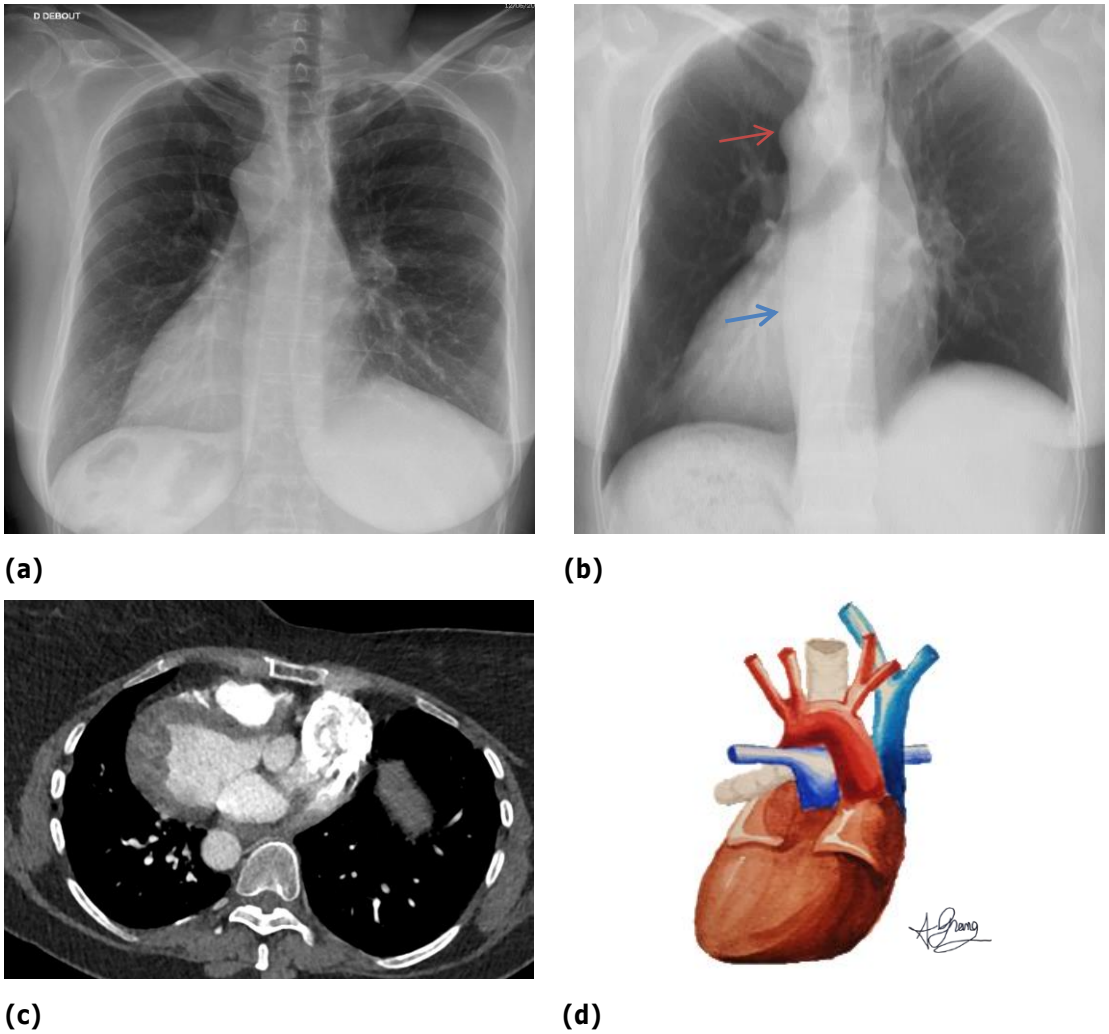

Fig. 3. Dextrocardia with situs inversus: On frontal chest X-ray **(a)** and coronal CT scan with MPVR reformatting (slice thickness: 128 mm) **(b)**, the aortic knob (red arrow) and the para-aortic line (blue arrow) are located on the right side of the mediastinum. The gastric air bubble is observed on the same side. Note the right-side marker (R) on the CXR, confirming correct image orientation. On axial CT scan in mediastinal window **(c)** the mediastinal structures are reversed, with a right-sided cardiac axis and the descending thoracic aorta located to the right of the vertebral column. Illustration **(d)** depicts this anatomical variant.

In case of dextrocardia without situs inversus, the aortic knob and the para-aortic line remain in their usual anatomical position on the left side of the mediastinum, while the cardiac axis is deviated to the right. The incidence of dextrocardia is estimated to be approximately 1 in 12,000 births (15).

1.3. Aortic arch variants

In its standard anatomical configuration, the aortic arch produces an indentation on the left lateral aspect of the trachea. A reversal of this tracheal indentation may suggest an anatomical variant of the aortic arch.

The right-sided aortic arch (fig. 4) is an anatomical variant in which the aortic arch courses along the right border of the trachea. It can be seen in 0.05% to 0.1% of chest radiographic examinations (16).

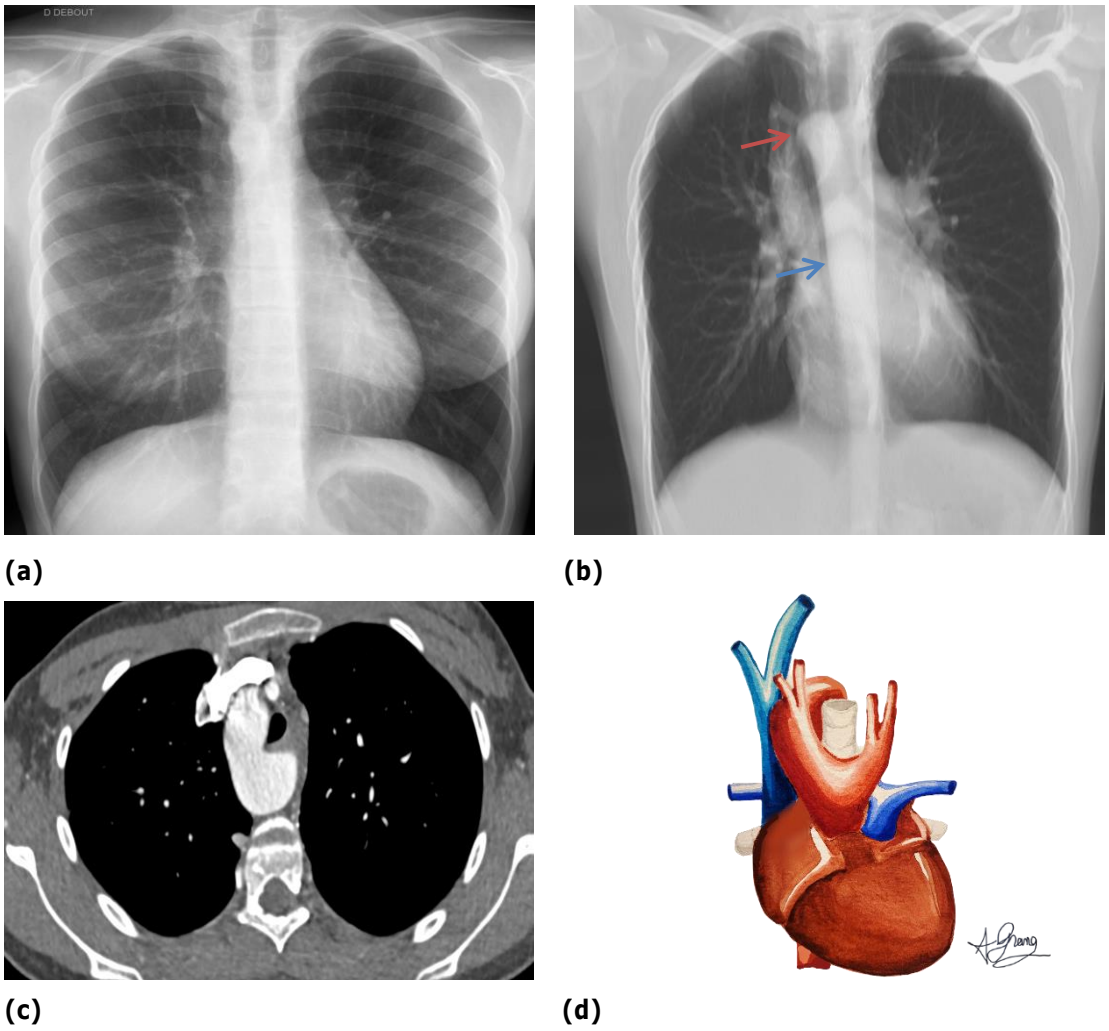

Fig. 4. A right-sided aortic arch appears, on CXR **(a)** and coronal CT scan with MPVR reformatting (slice thickness: 64 mm) **(b),** as a mass-like opacity in the right paratracheal region (red arrow) (17), with leftward tracheal displacement at the level of the arch. This variant is usually associated with a right descending thoracic aorta (blue arrow). Axial CT scan in mediastinal window **(c)** confirms the position of the aortic arch to the right of the trachea. Illustration **(d)** depicts a right aortic arch with mirror image branching which represents the most common subtype of right-sided aortic arch.

A double aortic arch (fig. 5) forms a complete vascular ring encircling both trachea and esophagus (18).

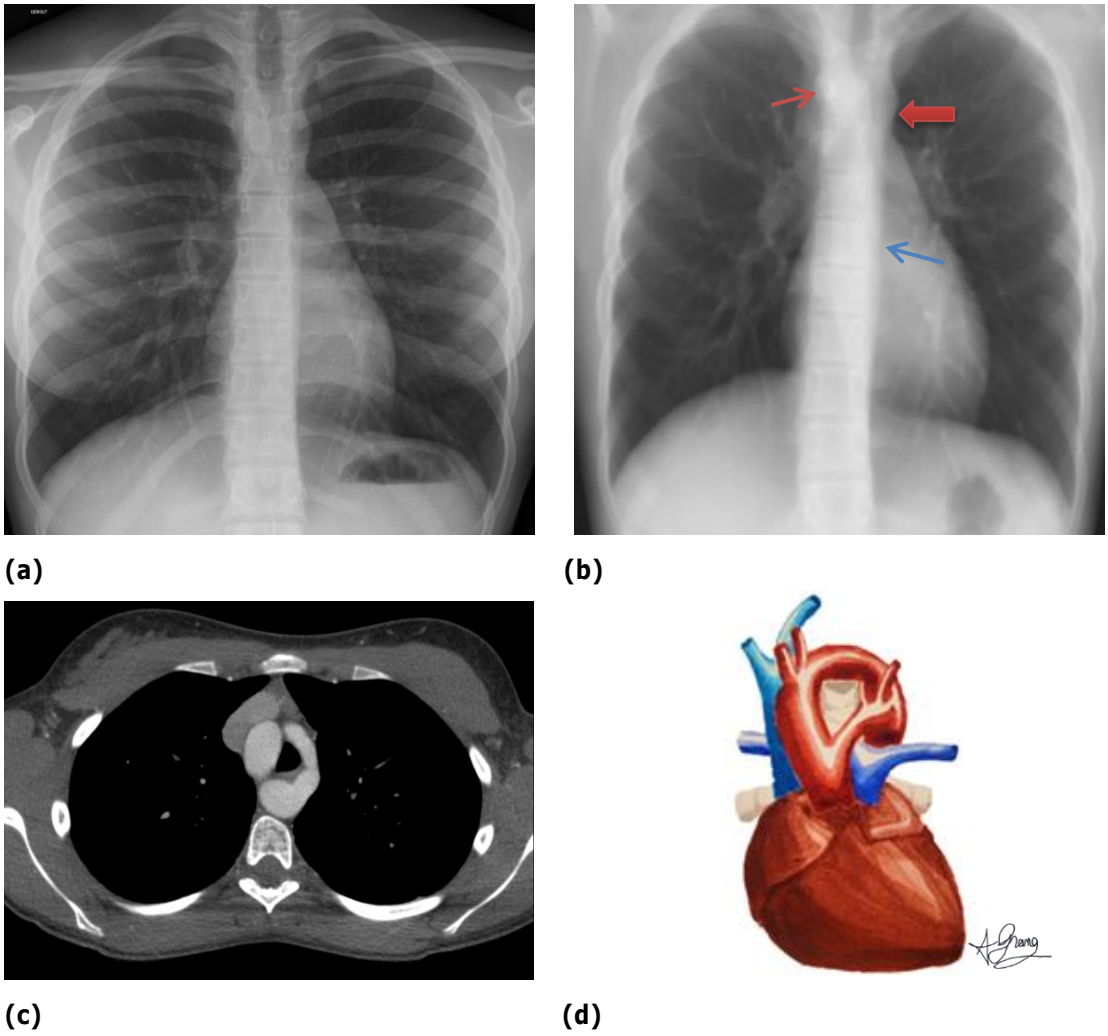

Fig. 5. Double aortic arch: on frontal chest X-ray **(a)** and coronal CT scan with MPVR reformatting (slice thickness: 128 mm) **(b)**, the right arch (thin red arrow) is typically larger and higher than the left (19), mimicking a right paratracheal mass. The trachea is deviated to the left. You can see the aortic button (thick red arrow) and the para-aortic line on the left (blue arrow). Axial CT scan in mediastinal window **(c)** and illustration **(d)** show the encirclement of the trachea by a double aortic arch — a configuration that explains the patient's symptoms, notably dyspnea.

1.4. Duplicated left superior vena cava (SVC)

Duplication of the superior vena cava (fig. 6) is the most common type of left-sided SVC anomaly. It is characterized by the presence of an additional left-sided SVC alongside the normal right-sided one. This anomaly occurs in 0.3% of the general population and in 10-11% of individuals with congenital heart disease (20). A duplicated left SVC (fig. 6) is not

easy to detect on CXR. One suggestive finding may be the presence of a central venous catheter with its tip abnormally positioned in the left paramediastinal area.

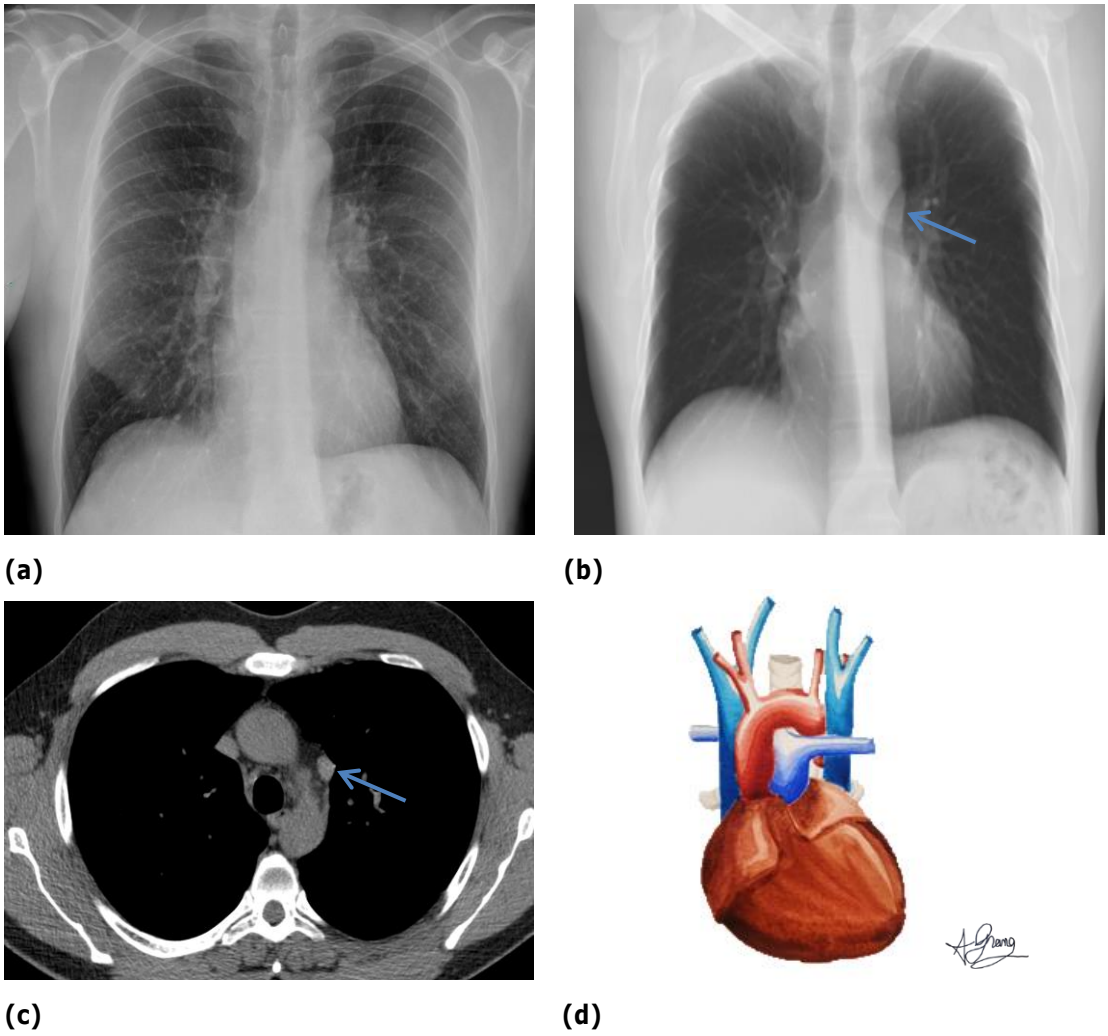

Fig. 6. Double superior vena cava: on frontal chest X-ray **(a)** and coronal CT scan with MPVR reconstruction (slice thickness: 128 mm) **(b)**, an additional vertical mediastinal line is visible, projected over the left pulmonary hilum and extending toward the aortic knob (blue arrow), corresponding to the left lateral wall of the left superior vena cava. On axial CT scan in mediastinal window **(c)**, the left superior vena cava is seen ascending laterally to the aortic arch, as illustrated in diagram **(d)**.

1.5. Azygos arch variants

The azygos arch (arcus venae azygos) is an important landmark to recognize in order to avoid mistaking it for a mediastinal lesion. It is visible at the level of T5–T6, above the right tracheobronchial angle, and superior to the right main bronchus. It is part of the normal anatomical boundaries of the mediastinum and typically measures less than 7 mm in thickness in the upright position. Variations of origin, course, tributaries, and termination of

the azygos system can alter its radiographic appearance (21). It can be contained within an accessory azygos fissure, an anatomical variant. An enlarged azygos arch (Fig. 7) can be seen in azygos continuation of the inferior vena cava (IVC), which has a prevalence of ~1.5% (range 0.2–3%) (22). In this case, the vertical portion of the azygos vein manifests as a right-sided vertical mediastinal interface. It is important to distinguish an enlarged azygos vein at the confluence with the SVC with a right-sided paratracheal mass or lymphadenopathy.

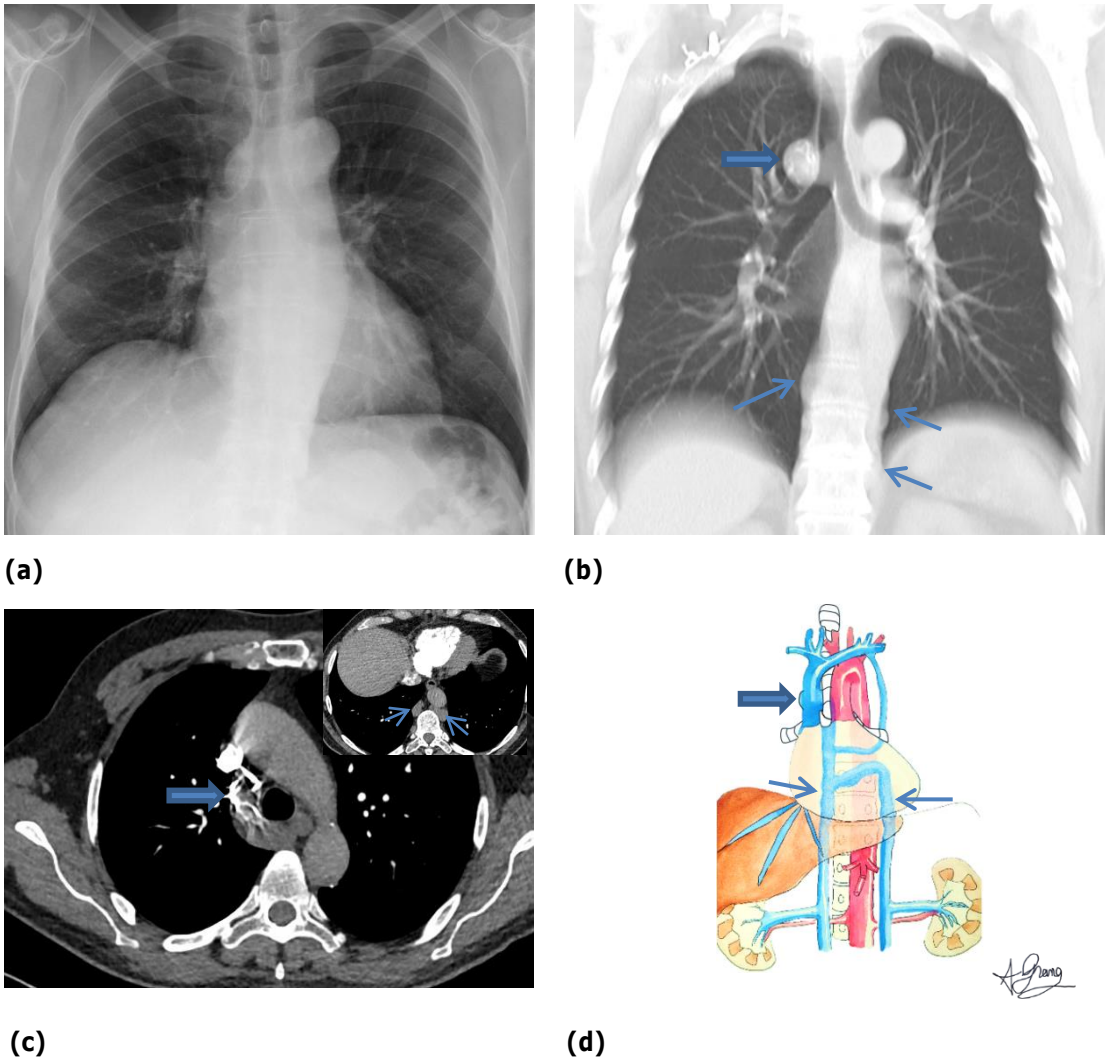

Fig. 7. On frontal chest X-ray **(a)** and coronal CT scan with MPVR reconstruction (slice thickness: 32mm) **(b)**, the mediastinum is widened and the azygos arch enlarged. As seen on axial CT scan in mediastinal window **(c)**, the azygos vein is dilated at the level of the azygos arch (thick blue arrow), located above the right tracheobronchial angle. It is important not to mistake this finding for a right-sided aortic arch, which would appear in a higher position (23). Note a subtle bilateral deviation of the paravertebral lines on the X-ray, more pronounced on the left side, giving them a wavy appearance, associated with moderate dilation of the accessory hemi-azygos vein (on the left) and the azygos vein (on the right) (thin blue arrows). Illustration **(d)** showing dilation of the azygos and hemiazygos veins, each continuing from a branch of a duplicated inferior vena cava, a configuration observed in cases of azygos continuation of the inferior vena cava.

1.6. Pulmonary arterial agenesis

Pulmonary arterial agenesis (fig. 8), also called congenital interruption of the pulmonary artery, is defined by the unilateral absence of the pulmonary artery. The space around the atretic pulmonary artery is filled with fibrofatty tissue and collateral vessels. On chest radiography, the main differential diagnosis is lung atelectasis. The estimated prevalence of pulmonary arterial agenesis is 1 in 200,000 (24).

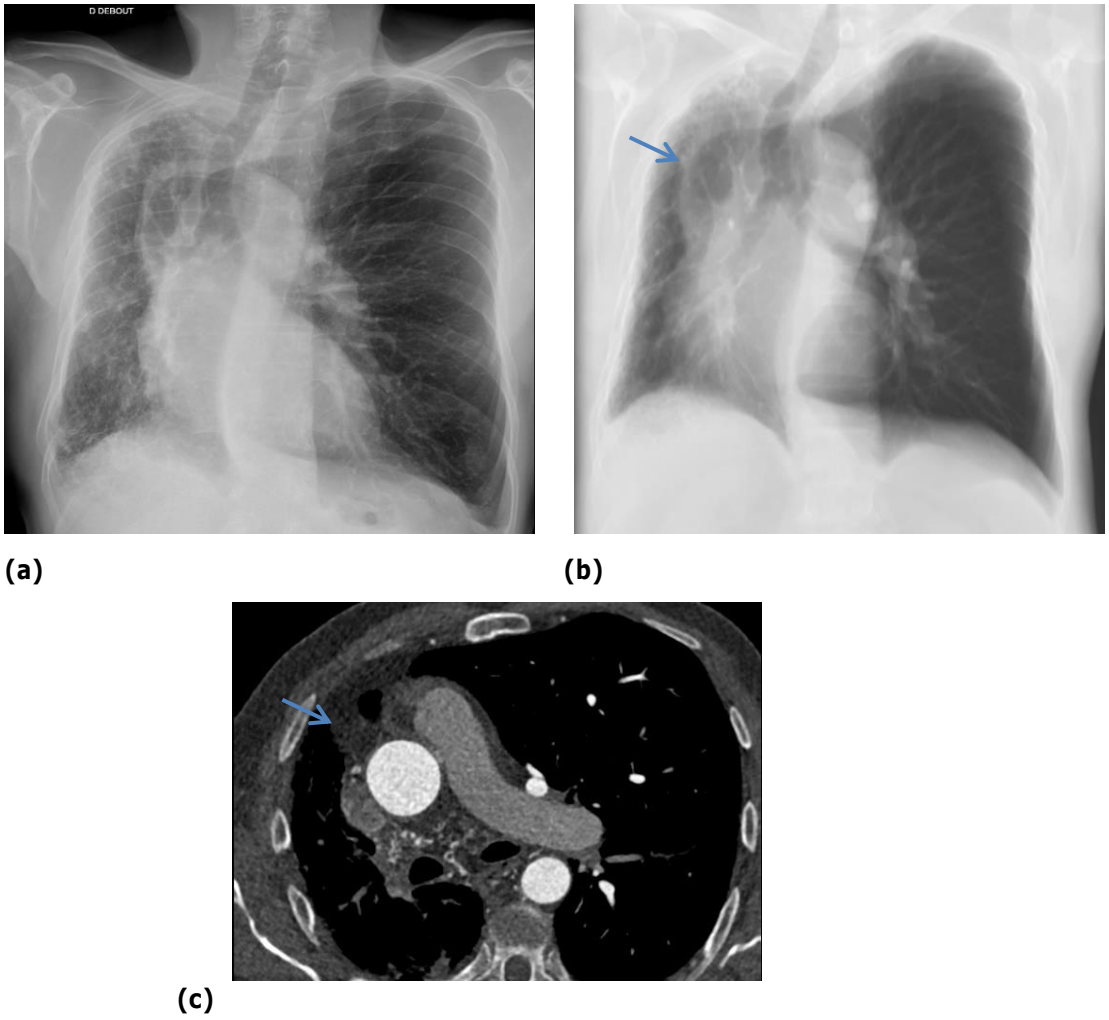

Fig. 8. A pulmonary arterial agenesis appears on CXR **(a)** and coronal CT scan with MPVR reformatting (slice thickness: 128 mm) **(b)**, as a small ipsilateral lung and hilum, and compensatory hyperinflation and herniation of the contralateral lung. Axial CT scan in mediastinal window **(c)** shows fibrous tissue adjacent to the pulmonary hilum, containing numerous small collateral vessels.
Note that this patient shows a significant shift of the anterior junction line toward the ipsilateral contracted hemithorax (discussed later) (blue arrow).

2. Perception of mediastinal lesions

Superimposed mediastinal lesions can alter the appearance of the normal mediastinum. In particular, they may cause displacement of normal mediastinal lines and stripes, which represent a transition zone between the mediastinum and the adjacent lung (fig. 9). Deviation of these structures can be subtle, and it is therefore essential not only to have a thorough knowledge of normal mediastinal lines, but also to perform a meticulous visual assessment.

Localization of a mediastinal lesion on CXR involves a two-step approach. The first part is to assess whether the lesion is truly mediastinal (deviation of mediastinal lines being a strong argument supporting it) and the second part is to place it in the anterior, middle, or posterior mediastinum. The specific displacement of a given line can provide valuable information about the likely location of the lesion within the mediastinum.

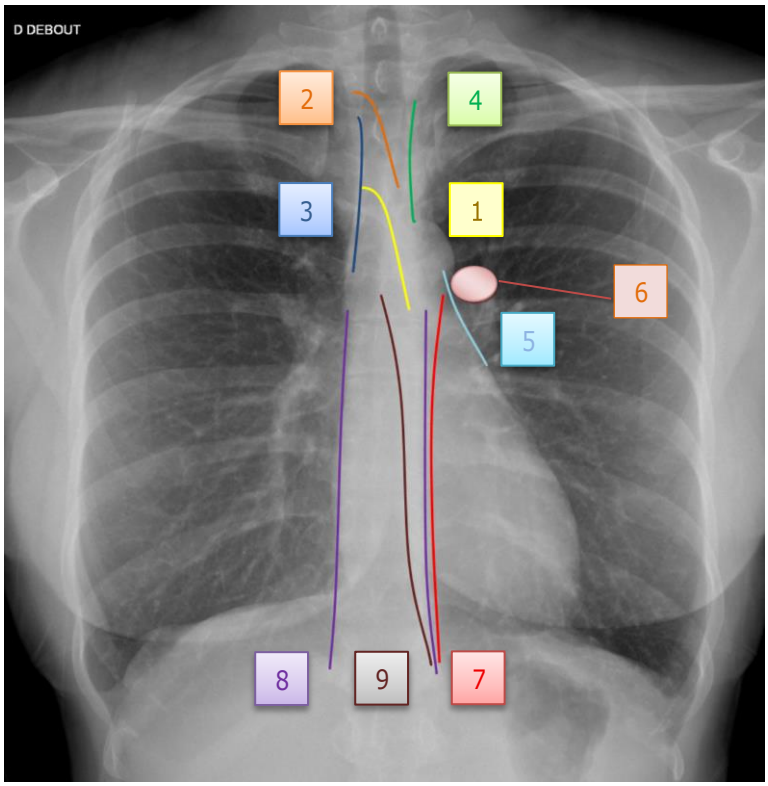

Fig. 9. Key médiastinal lines and stripes :

1. Anterior junction line
2. Posterior junction line
3. Right paratracheal stripe
4. Left paratracheal stripe
5. Aortic-pulmonary stripe
6. Aortopulmonary window
7. Descending aorta line
8. Right and left paraspinal lines
9. Azygoesophageal stripe

2.1. Anterior junction line

The anterior junction line can be seen in approximately 40% of upright CXR (10). The anterior junction line corresponds to the apposition of the pleural layers of both lungs along the anterior mediastinum, above the level of the cardiac silhouette. Its deviation may be caused by an underlying mass in that region (fig. 10) (25). But it can also result from atelectasis or hyperinflation of the adjacent lung parenchyma (as shown in figure 8).

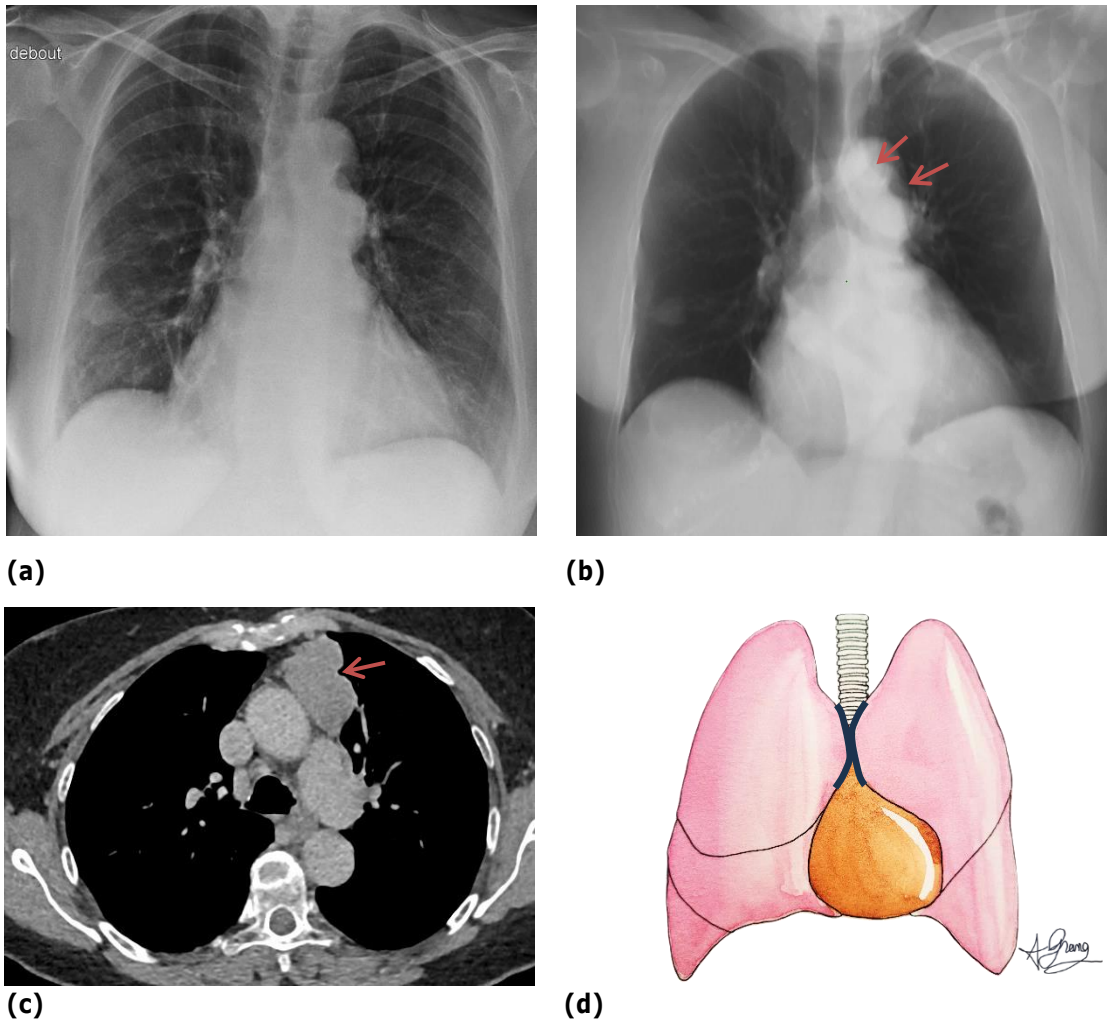

Fig. 10. On frontal chest X-ray **(a)** and coronal CT scan with MPVR reconstruction (slice thickness: 128 mm) **(b)**, a deviation of the anterior junction line (red arrows) is observed. Although difficult to identify on the chest X-ray, a well-defined area of increased opacity is visible projecting from the medial aspect of the aortic knob (arrows), corresponding to an anterior mediastinal mass responsible for displacement of this line. The diagnosis is confirmed on axial CT scan in mediastinal window **(c)**. This mass turned out to be a thymoma in a patient with myasthenia gravis. Diagram **(d)** illustrates normal anatomical configuration of the anterior junction line.

2.2. Posterior junction line

The posterior junction line has been reported in approximately 32% of normal upright CXR (25). This line represents the apposition of the pleural surfaces of the upper lobes along the posterior mediastinum. Displacement, convex contour, or disappearance of this posterior junction line (when visible on prior imaging in the same patient) may suggest the presence of a posterior mediastinal mass (fig. 11). As with the anterior junction line, volume loss or hyperinflation of the surrounding lung can also cause deviation of this line (26-28).

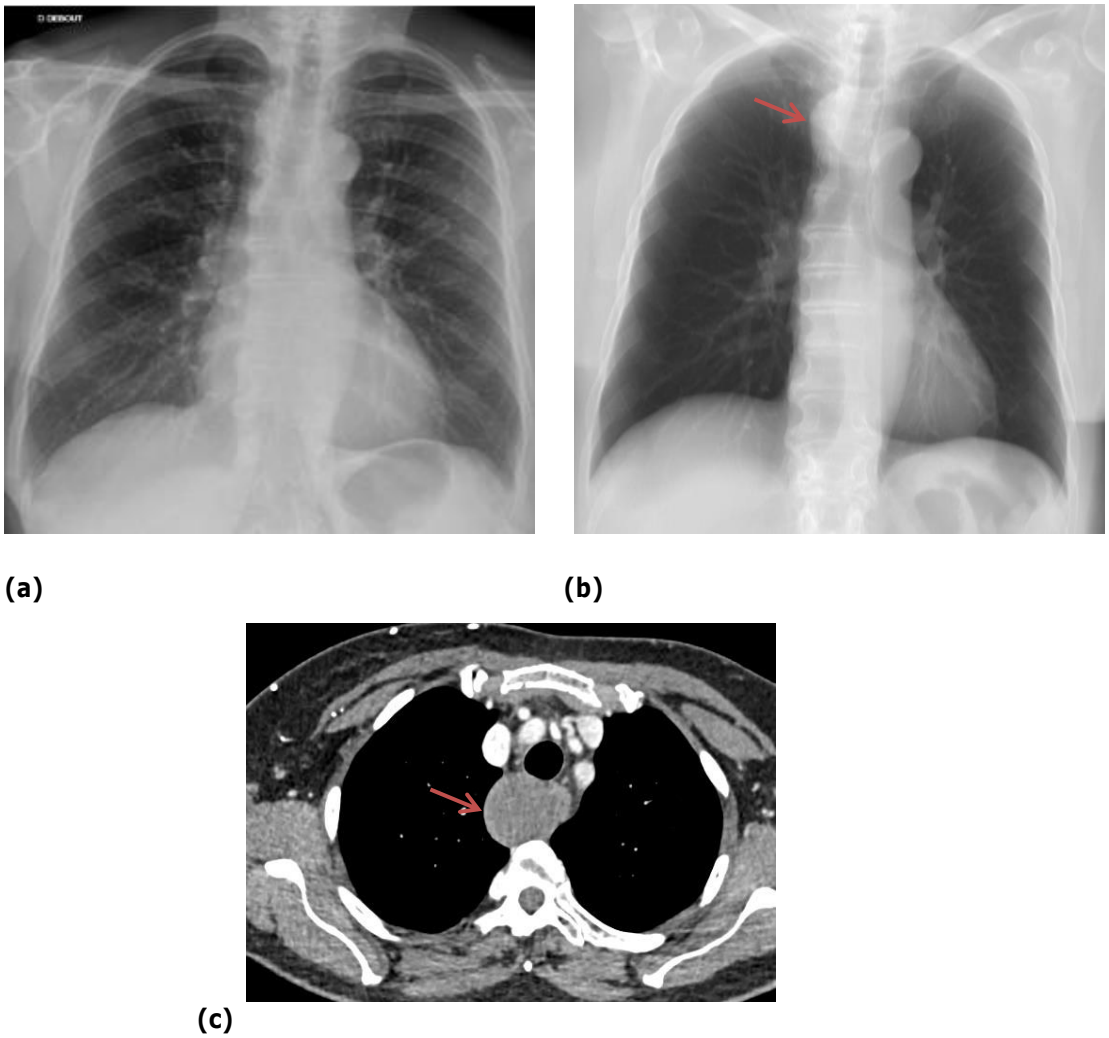

(a) **(b)**

(c)

Fig. 11. Frontal chest X-ray **(a)** and coronal CT scan with MPVR reformatting (slice thickness: 128 mm) in the lung window **(b)** show a well-defined mass (red arrows) causing rightward deviation of the posterior junction line (no mass effect is observed on the right tracheal margin). Axial CT scan in mediastinal window **(c)** reveals a fluid-filled lesion consistent with a bronchogenic cyst.

2.3. Right paratracheal stripe

The right paratracheal stripe (fig. 12) is the most commonly seen mediastinal stripe, visible on 97% of CXR. It has a normal maximum thickness of 4 mm (25). It extends inferiorly to the right tracheobronchial angle at the level of the azygos arch. Physiologically, it is thickened at the level of the azygos arch, which forms an oval-shaped structure.

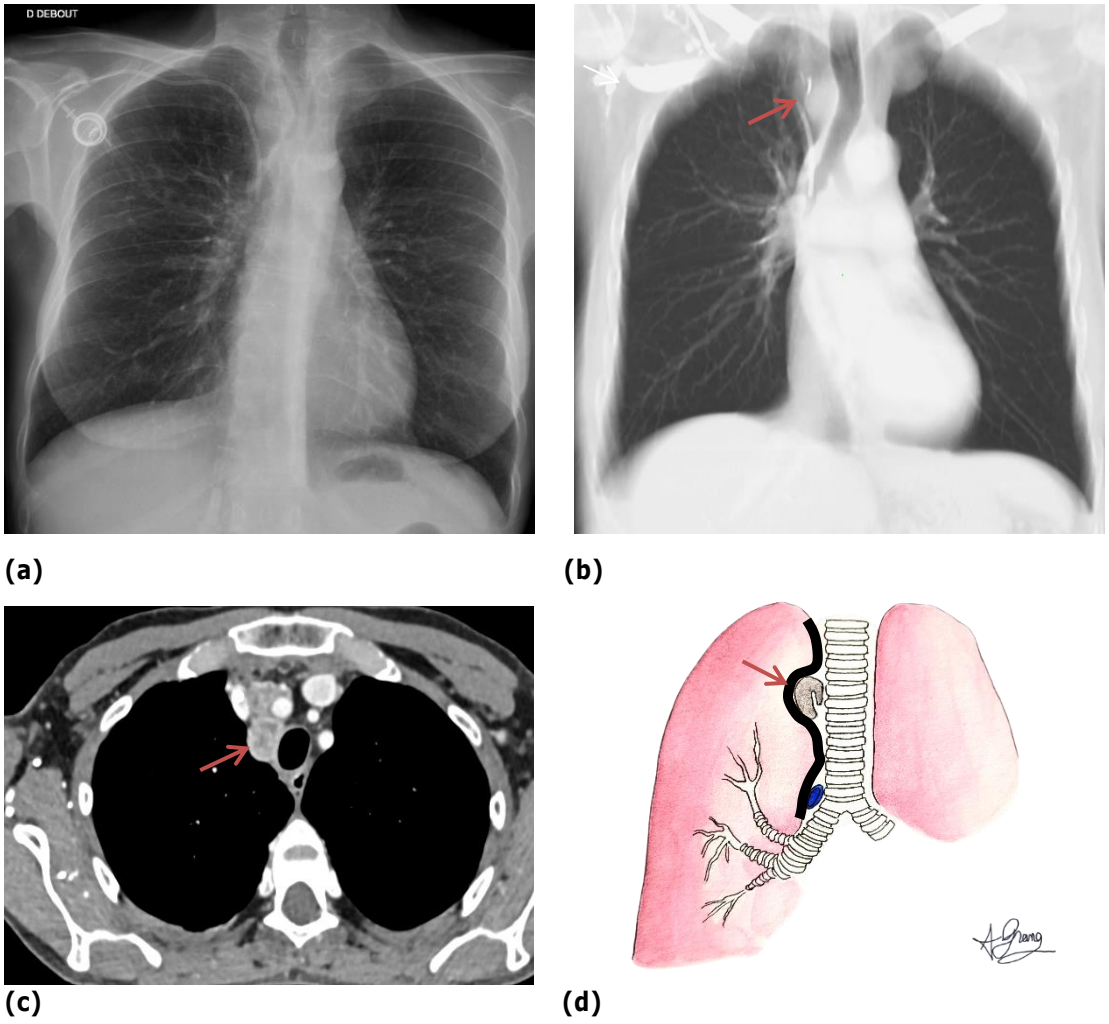

Fig. 12. On frontal chest X-ray **(a)** and coronal CT scan with MPVR reconstruction (slice thickness: 32 mm) **(b)**, a right upper paratracheal lesion (red arrow) is visible, associated with contralateral tracheal deviation. On axial CT scan in mediastinal window **(c)**, this lesion corresponds to a mediastinal lymphadenopathy. Diagram **(d)** illustrates the displacement of right paratracheal stripe by a lymph node (arrow). The blue ovoid structure corresponds to the azygos vein arch.

2.4. Left paratracheal stripe

The left paratracheal stripe is visible on 21%–31% of CXR (25, 29). This line extends from the left subclavian artery to the aortic arch.

2.5. Aortic-pulmonary stripe

The aortic-pulmonary stripe corresponds to the interface between the left upper lobe and the mediastinal border, from the aortic arch superiorly to the left pulmonary artery inferiorly (29). It delineates the anterior margin of the aortopulmonary window. This stripe appears linear or may also be subtly convex (26, 30-31). It can be displaced by an anterior mediastinal mass or a pneumomediastinum (fig. 13).

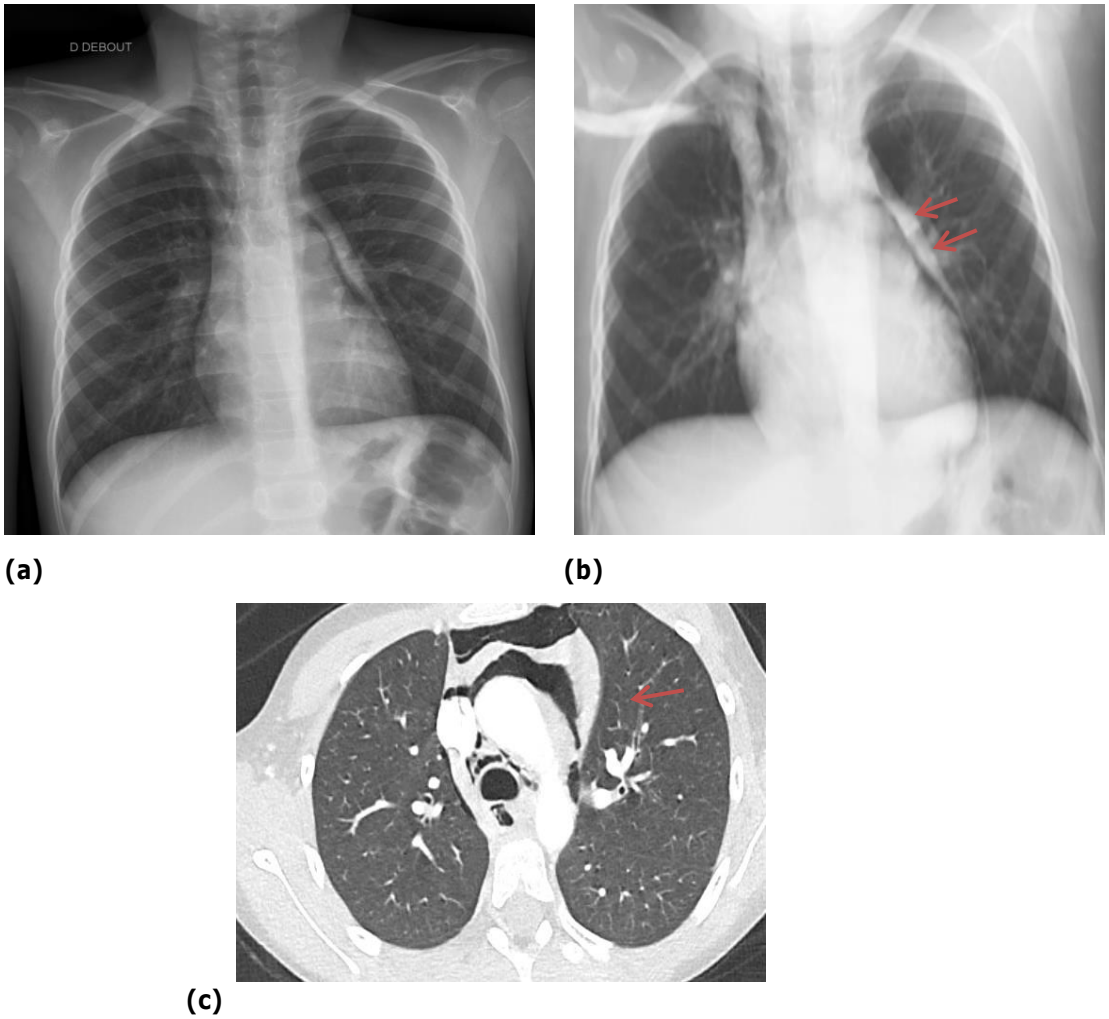

Fig. 13. Frontal chest X-ray **(a)** and coronal CT scan with MPVR reformatting (slice thickness: 128 mm) **(b)** show the aorto-pulmonary stripe (red arrows) made visible by the presence of an underlying pneumomediastinum. On axial CT scan in lung window **(c)**, the pneumomediastinum is seen along the left lateral aspect of the aortic arch.

2.6. Aortopulmonary window

Aortopulmonary window is a mediastinal space located between the aortic arch and the left pulmonary artery on frontal CXR (28, 31). It lies posterior to the aortic-pulmonary stripe, bounded by the aortic arch above, the left pulmonary artery below, the ascending aorta in front, and the descending aorta behind. Medially, it is bordered by the trachea, the left main bronchus, and the esophagus (28, 31). A convex contour of the aortopulmonary window is considered abnormal (fig. 14) (10). In the context of left vocal cord paralysis, the aortopulmonary window is a critical area to examine carefully for any underlying mass effect, as the left recurrent laryngeal nerve passes through it (25-26, 31).

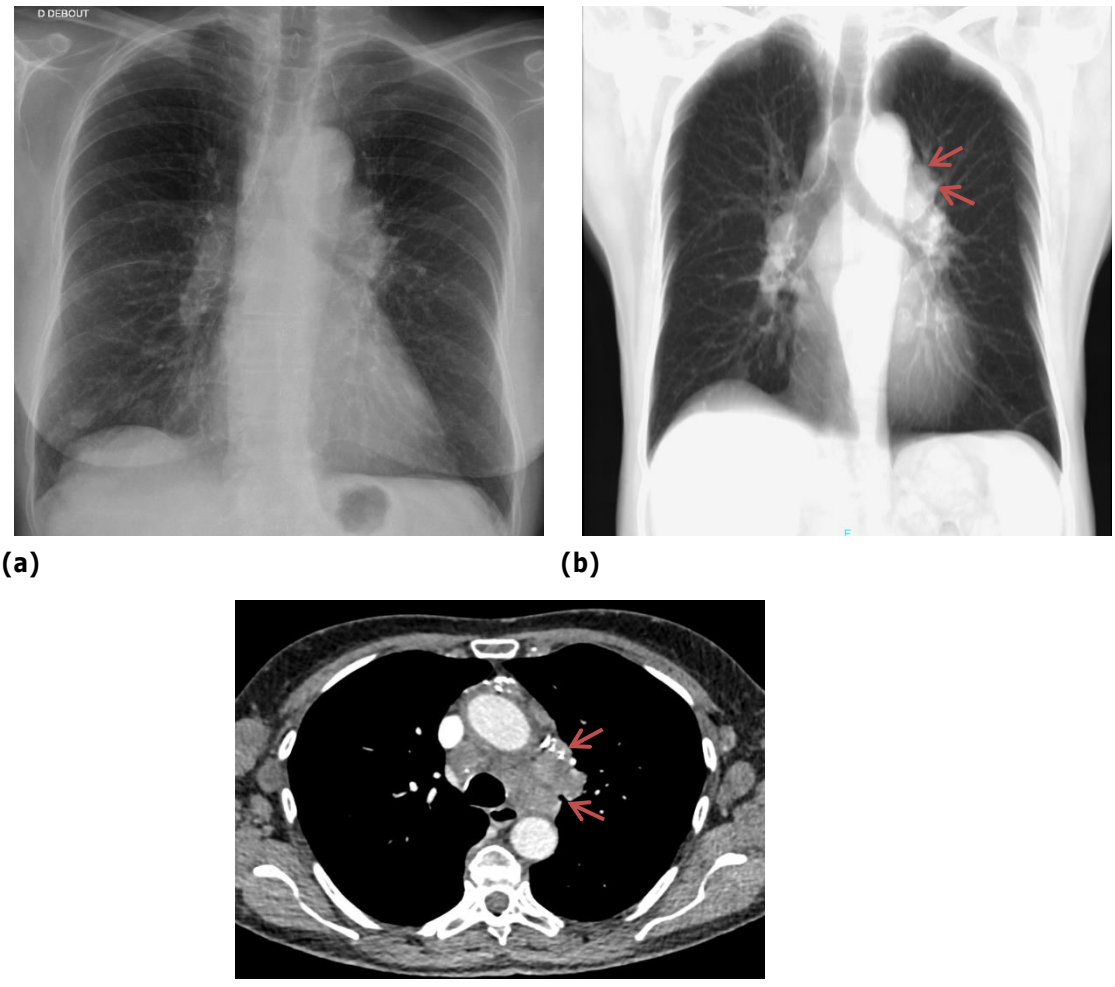

Fig. 14. A mass effect filling the aorto-pulmonary window (red arrows), producing an abnormal convex contour, is visible on frontal chest X-ray **(a)** and on coronal CT scan with MPVR reformatting (slice thickness: 64 mm) **(b)**. On axial CT scan in mediastinal window **(c),** there is a nodal mass in the aortopulmonary window, consistent with non-Hodgkin lymphoma.

2.7. Descending aorta line

In some patients, the left para-aortic line and the left paravertebral line may converge. Deviation or reduced visibility of the para-aortic line may suggest an abnormality of the descending thoracic aorta. A potential pitfall is that significant tortuosity of the thoracic aorta can mimic an aortic aneurysm or a mediastinal mass (fig. 15) (32). If such doubt exists on the chest radiography, thoracic CT angiography should be performed to clarify the diagnosis (23).

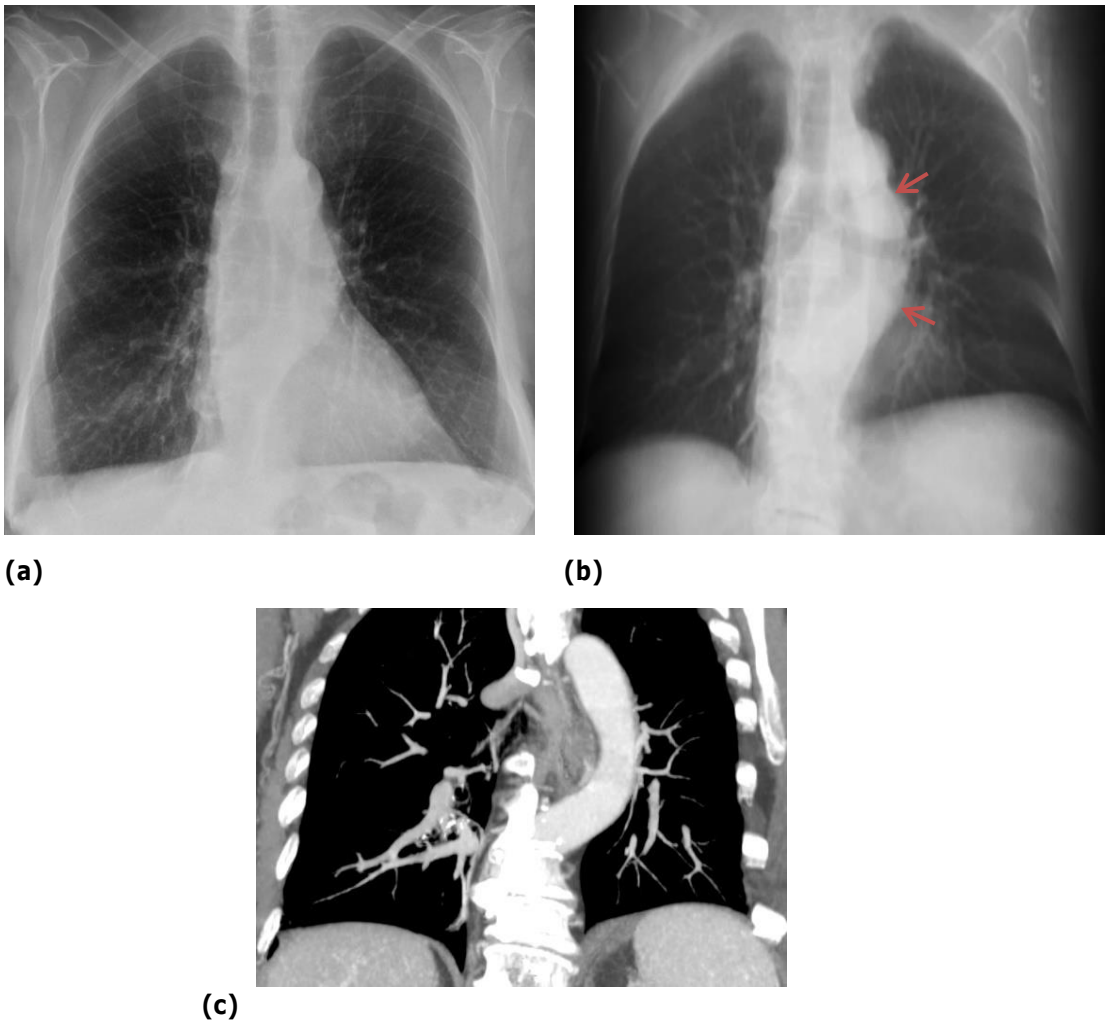

(a) **(b)**

(c)

Fig. 15. Frontal chest X-ray **(a)** and coronal CT scan with MPVR reformatting (slice thickness: 128 mm) **(b)** give the impression of a mediastinal mass or aneurysmal dilatation of the aorta. Coronal CT scan in mediastinal window with MIP reformatting (slice thickness: 16 mm) **(c)** reveals that this appearance is due to significant tortuosity of the descending thoracic aorta (red arrows).

2.8. Right and left paraspinal lines

Despite its name, the paraspinal line is not a true anatomical line but rather represents an interface between tissues of differing densities. Its visibility may be enhanced — or sometimes entirely dependent on — an optical phenomenon known as the Mach band effect, which can create the illusion of a sharper boundary than actually exists (33). The left paravertebral line is more frequently seen than the right. Paraspinal lines are observed in approximately 23% of cases on the right side and 41% on the left side (fig. 16) (25-26). This is related to the descending thoracic aorta which promotes a tangential orientation of the left paravertebral line to the X-ray beam (10).

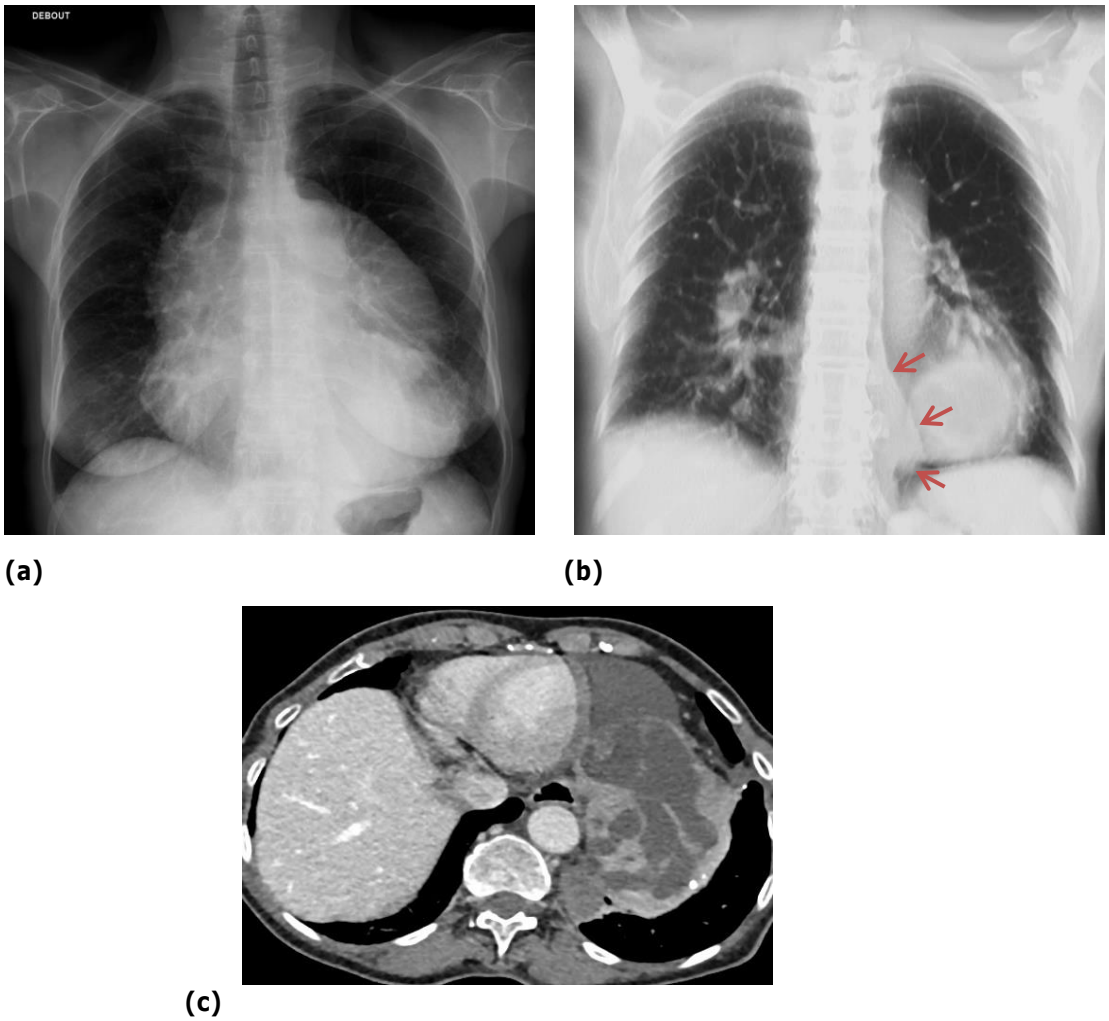

(a) **(b)**

(c)

Fig. 16. A large mediastinal enlargement associated with a solitary fibrous tumour of the pleura is clearly visible on frontal chest X-ray **(a)**. However, more subtle is the deviation of the left paravertebral line (red arrows) which is better appreciated on coronal CT scan with MPVR reformatting (slice thickness: 32 mm) **(b)**. This deviation is linked to a second tumour, visible on axial CT scan in mediastinal window **(c)**. When carefully analyzed, the deviated paravertebral line converge towards the spine below the level of the diaphragmatic cupola, confirming the thoracic origin of the lesion (negative thoraco-abdominal sign, described later).

2.9. Azygoesophageal stripe

The azygoesophageal recess is not considered a true mediastinal stripe, but it remains an interface that should be carefully analyzed. It is formed by the medial border of the right lower lobe coming into contact with the posterior mediastinum, particularly the esophagus. It extends vertically from the anterior curve of the azygos vein to the aortic hiatus (26). Abnormal convexity of this stripe is most frequently associated with an esophageal abnormality (25) but it may also be related to lymphadenopathy, left atrial enlargement, hiatal hernia, or a bronchopulmonary foregut malformation (fig. 17).

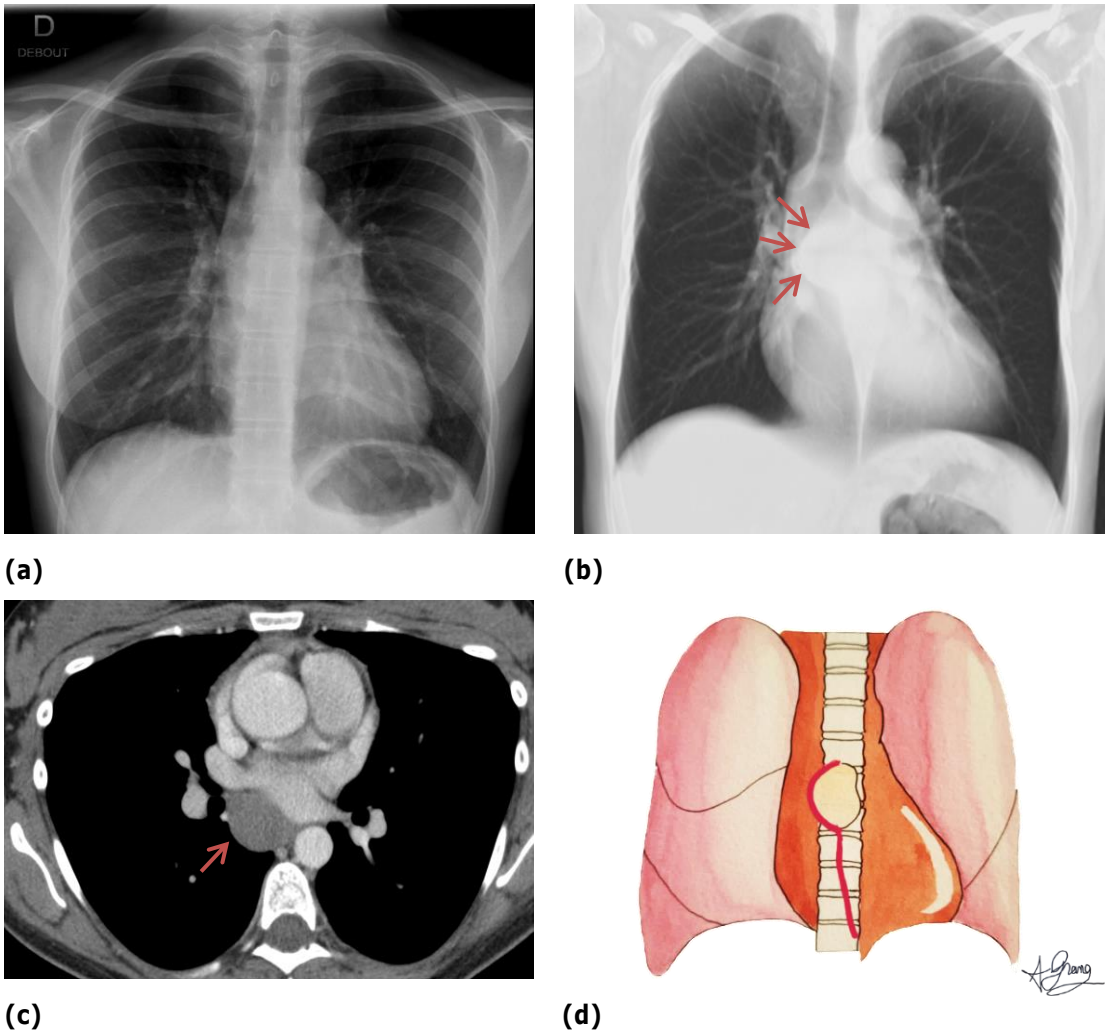

Fig. 17. Frontal chest X-ray **(a)** and coronal CT scan with MPVR reformatting (slice thickness: 64 mm) **(b)** reveal a deviation of the upper third of the azygoesophageal stripe, which appears convex to the right. This finding is related to a fluid-filled lesion observed on axial CT scan in mediastinal window **(c)**, consistent with a subcarinal bronchogenic cyst. This lesion is illustrated on diagram **(d)**.

2.10. Subcarinal space

The subcarinal space is a fat-containing space located between the carina superiorly, the left atrium inferiorly, and the two main bronchi laterally. The carinal angle normally measures between approximately 52° and 68° (34) and may be widened in the presence of lymphadenopathy, esophageal mass (fig. 18), or left atrial enlargement, for example.

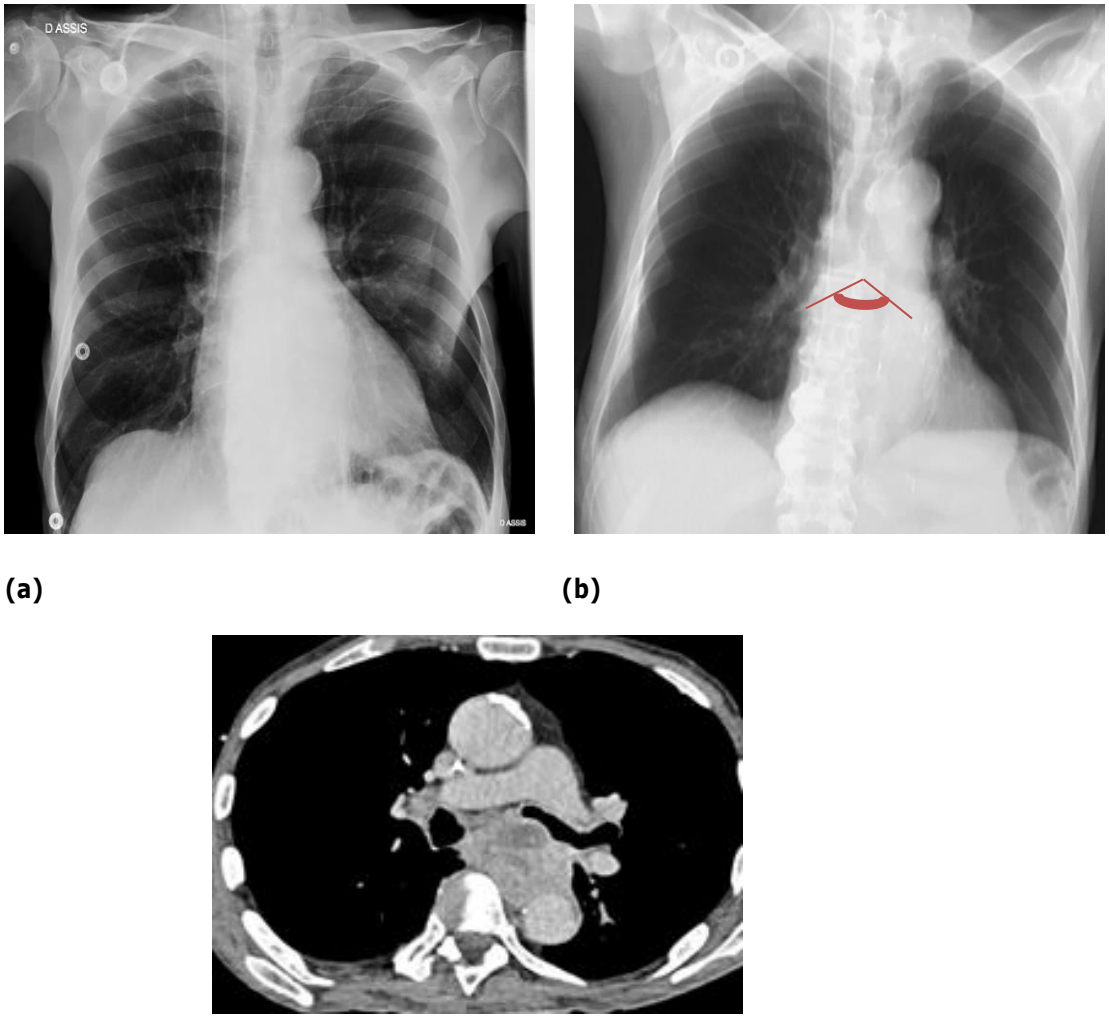

(a) **(b)**

(c)

Fig. 18. CXR **(a)** and coronal CT scan with MPVR reformatting (slice thickness: 128 mm) **(b)** depict a marked widening of the subcarinal angle (>90°), with evidence of a mass effect on the origin of the main bronchi. On axial CT scan in mediastinal window **(c)**, a posterior mediastinal mass is visible, consistent with an esophageal tumor.

3. Blind spots or hidden areas

Several areas on chest radiographs are known to be more challenging to evaluate, and it is not uncommon for superimposed lesions to be overlooked in these regions. These include the lung apices, hilar regions, retrocardiac space, and the lung bases projected over the diaphragmatic domes. These areas represent significant sources of observational error (35).

3.1. Lung apices

The pulmonary apex is a problematic area to assess due to the superimposition of numerous normal anatomical structures, which physiologically increase the opacity of this region. These include clavicles, first ribs, transverse processes of the thoracic vertebrae, and supra-aortic vessels. Such superimpositions result in reduced contrast between potential lesions and the adjacent pulmonary parenchyma, making detection more difficult (fig. 19).

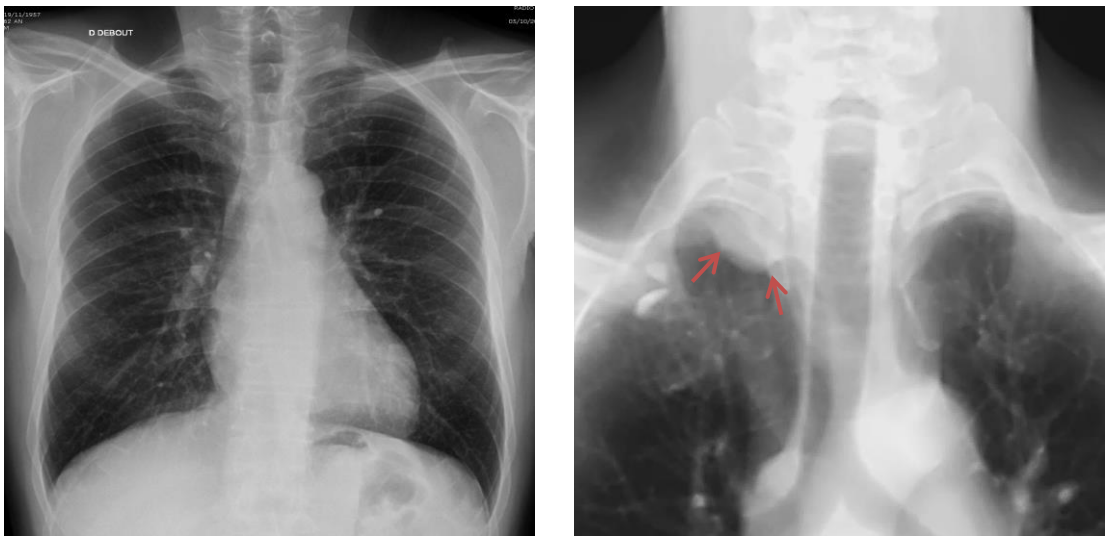

(a) **(b)**

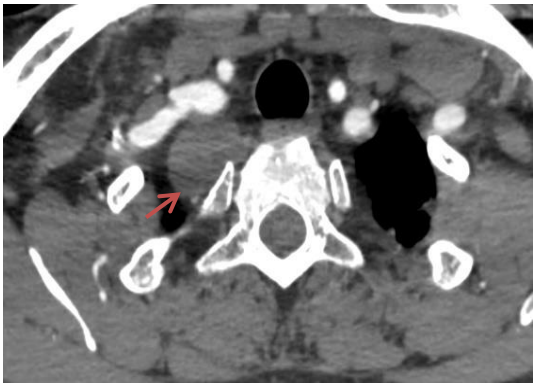

(c)

Fig. 19. On frontal chest X-ray **(a)** and CT scan of the supra-aortic trunks (SAT) in coronal section with MPVR reformatting (slice thickness: 64 mm) **(b)**, close inspection of the apical region of the right upper lobe reveals a lesion that appears to be extrapulmonary and posteriorly located (its position can be determined using the cervicothoracic sign, detailed later). On axial SAT CT scan **(c)** in mediastinal window, this lesion corresponds to a well-defined nodular formation, compatible with a schwannoma.

3.2. Hilar regions

The pulmonary hilum is a region of limited visibility on chest radiography because it contains numerous overlapping vascular structures, such as the pulmonary arteries and veins. This anatomical complexity makes it difficult to detect any superimposed lesion (fig. 20). Vessels seen in cross-section at the hilum may even mimic pulmonary nodules, potentially leading to unnecessary additional CT imaging.

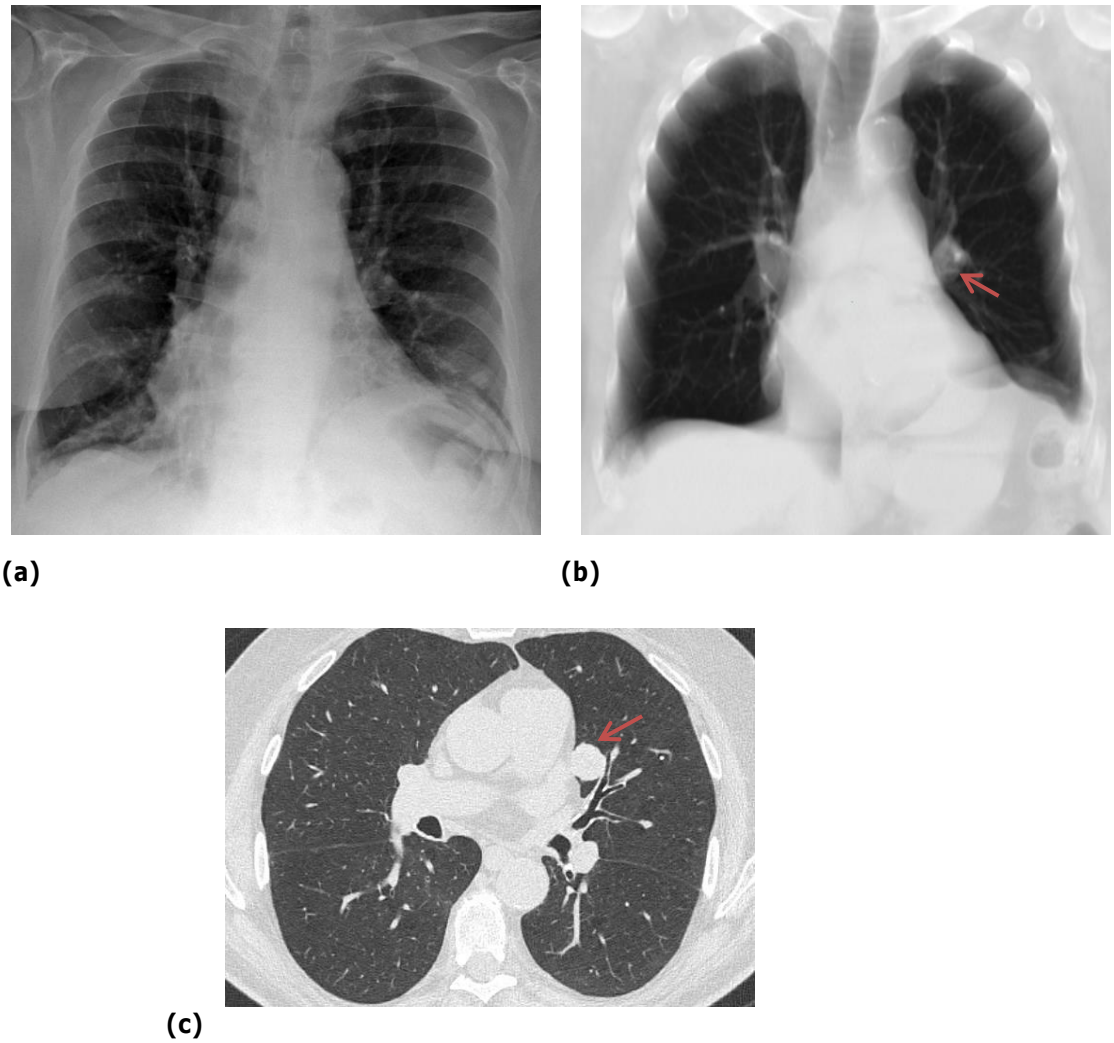

(a) **(b)**

(c)

Fig. 20. A nodular opacity is seen adjacent to the lower portion of the left pulmonary hilum (red arrow) on frontal chest X-ray **(a)** and is confirmed on coronal CT scan with MPVR reformatting (slice thickness: 64 mm) **(b)** and on axial CT scan in lung window **(c)**.

3.3. Retrocardiac region

The retrocardiac area is also challenging to assess due to increased opacity of the pulmonary field in this region, resulting from the superimposition of the cardiac silhouette (fig. 21).

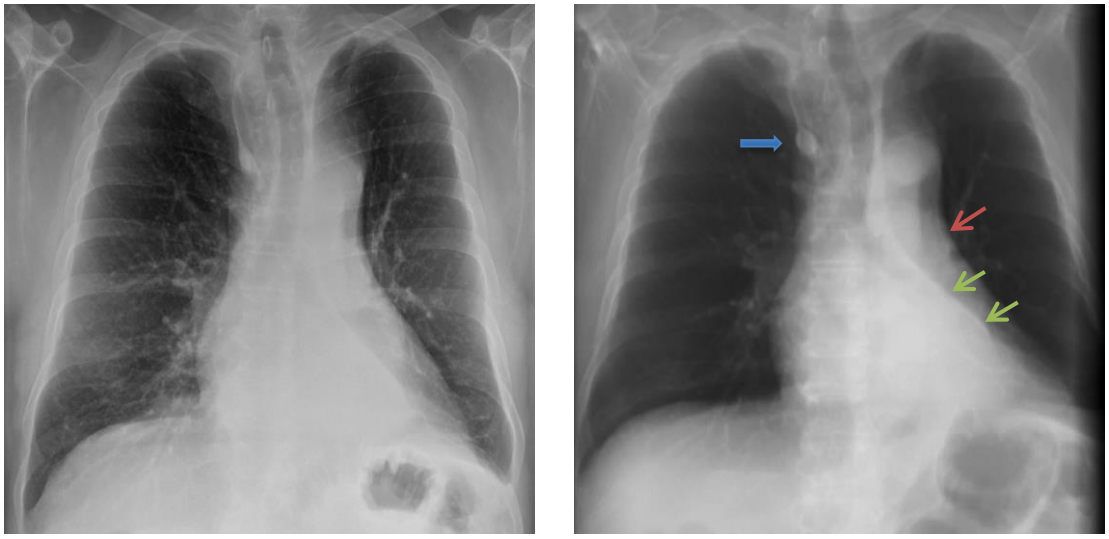

(a) **(b)**

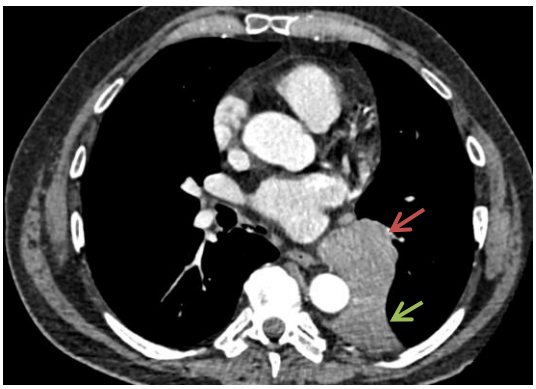

(c)

Fig. 21. A triangular opacity with well-defined margins (green arrows), visible in the retrocardiac region, is seen on both X-ray **(a)** and coronal CT scan with MPVR reformatting (slice thickness: 128 mm) **(b)**. It is associated with volume loss in the left lung field compared to the contralateral side, suggesting left lower lobe atelectasis. Additionally, the left pulmonary hilum appears significantly more prominent than the right (red arrow), raising suspicion of an underlying mass, likely responsible for the atelectasis. This hypothesis is confirmed on axial CT scan in mediastinal window **(c)**. Note the presence of an azygos scissure (thick blue arrow).

4. Identification of key signs for the localization of thoracic opacities

After identifying a thoracic opacity on a CXR, recognizing specific radiographic signs is essential to accurately localize it and increase diagnostic confidence.

4.1. Silhouette sign

The silhouette sign is somewhat misleading as it is considered positive when a normal silhouette disappears. It is sometimes more accurately referred to as "loss of silhouette sign" or "loss of outline sign". This sign occurs when a lesion lies in the same plane and is in direct anatomical contact with mediastinal or diaphragmatic structure, resulting in obscuration of its border (36).

Thus, the silhouette sign can help localize abnormalities within the chest. The main lines and contours that may be obscured —highlighted in bold below — depend on the location of the opacity, which is indicated in italics:

Concerning the right lung field:

- ***Right paratracheal stripe*** *- Right upper lobe/anterior mediastinum (fig. 22).*
- ***Right heart border (right atrium)*** *- Right middle lobe (fig. 23).*
- ***Right hemidiaphragm*** *- Right lower lobe.*

Regarding the left hemithorax:

- ***Aortic knuckle*** *- Left upper lobe/middle mediastinum (fig. 24).*
- ***Left heart border*** *(left ventricle) – Lingula (fig. 25).*
- ***Descending aorta*** *- Left lower lobe.*
- ***Left hemidiaphragm*** *- Left lower lobe.*

In relation with both lung fields:

- ***Paraspinal lines*** *- Medial lung/Posterior mediastinum.*

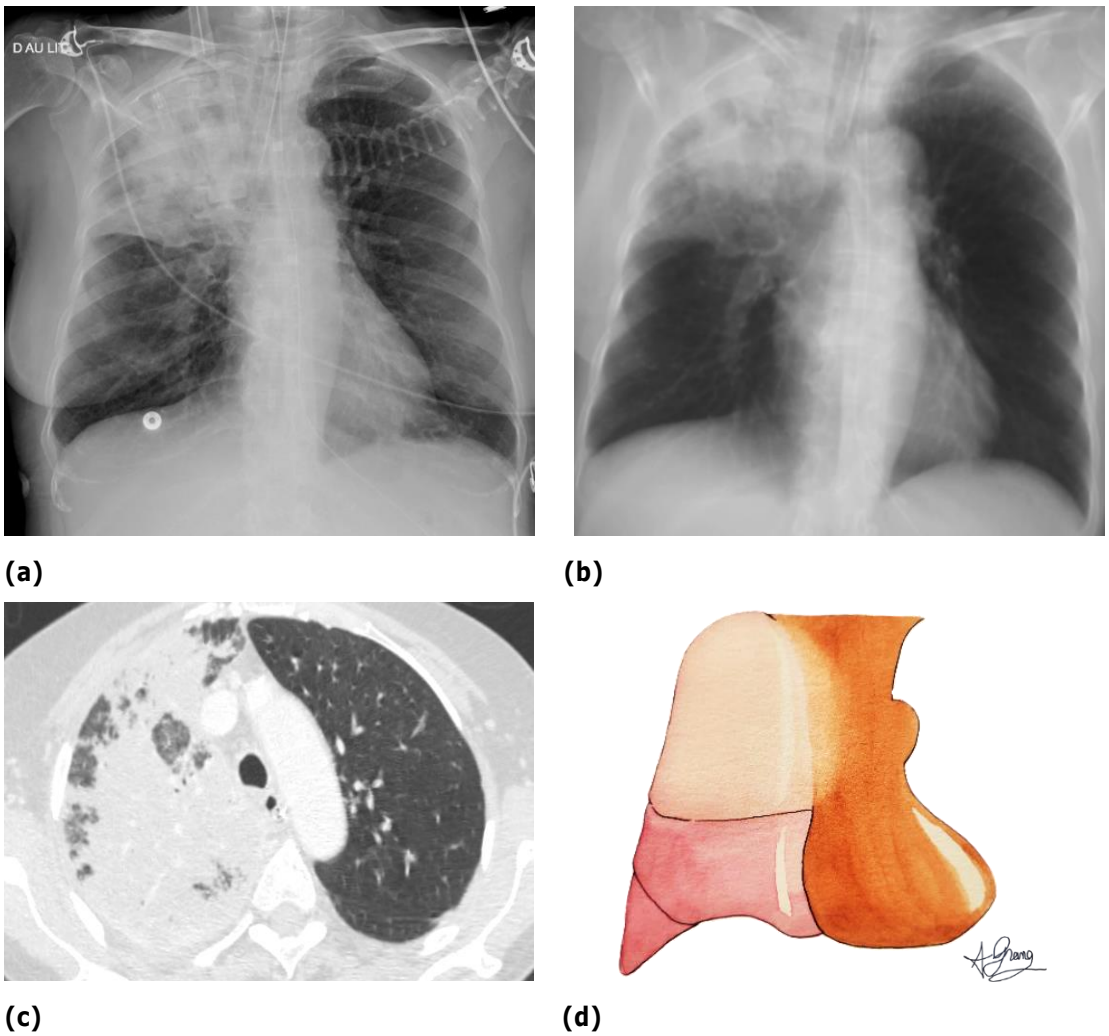

(a) **(b)**

(c) **(d)**

Fig. 22. Frontal chest X-ray **(a)** and coronal CT scan with MPVR reformatting (slice thickness: 128 mm) **(b)** depict an acute right upper lobe lobar pneumonia outlining the minor fissure and obscuring the right paratracheal stripe. On axial CT scan in lung window **(c)**, the consolidation is seen in direct contact with the right lateral border of the trachea, explaining its obscuration on the chest X-ray. This sign is illustrated in diagram **(d)**.

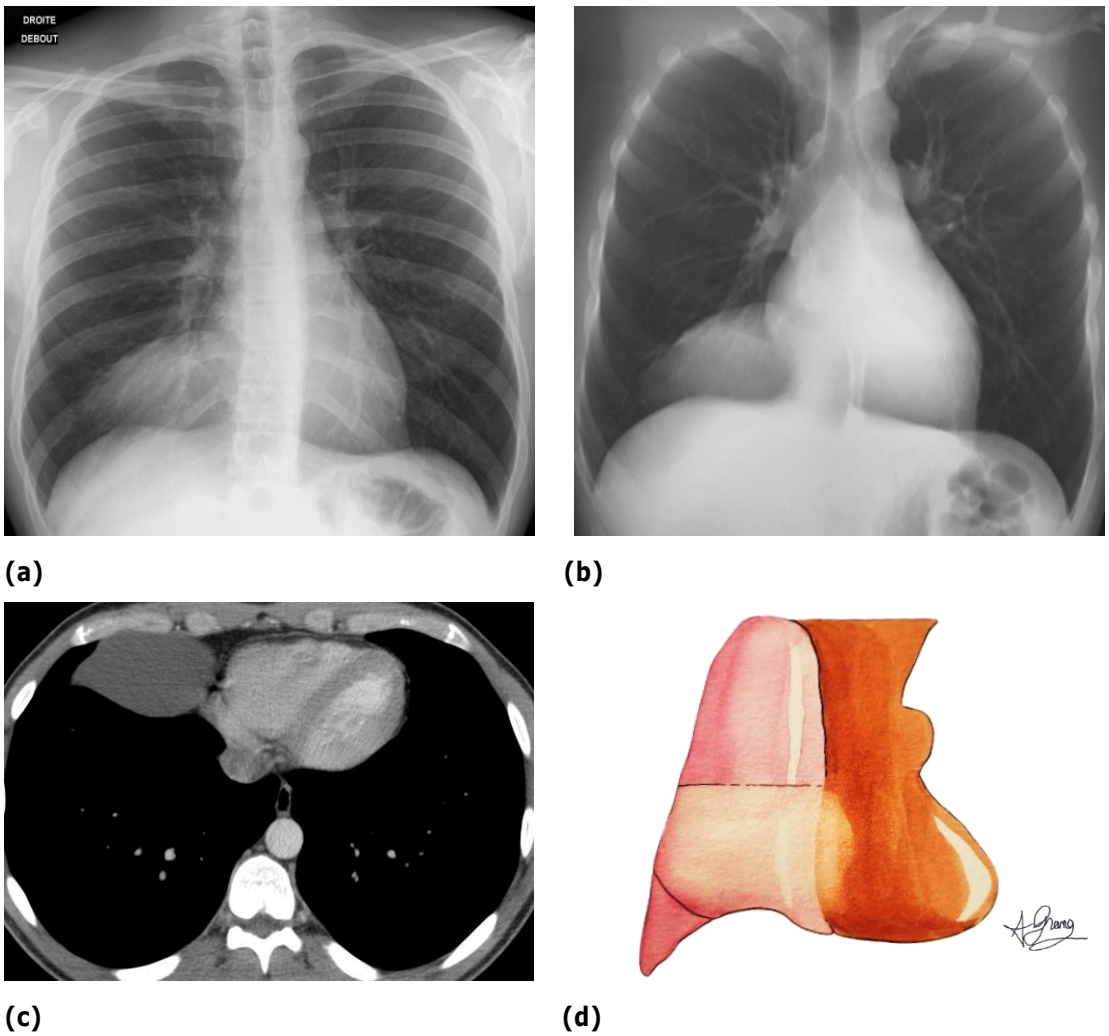

Fig. 23. Frontal chest X-ray **(a)** and coronal CT scan with MPVR reformatting (slice thickness: 128 mm) **(b)** show a right inferior paramediastinal lesion partially effacing the right heart border, suggesting a paracardiac origin. In addition, the diaphragmatic dome remains visible, supporting an anterior origin of the lesion. Axial CT scan in mediastinal window **(c)** reveals a fluid component. This appearance is consistent with a pleuropericardial cyst. The positive silhouette sign is illustrated in diagram **(d)**.

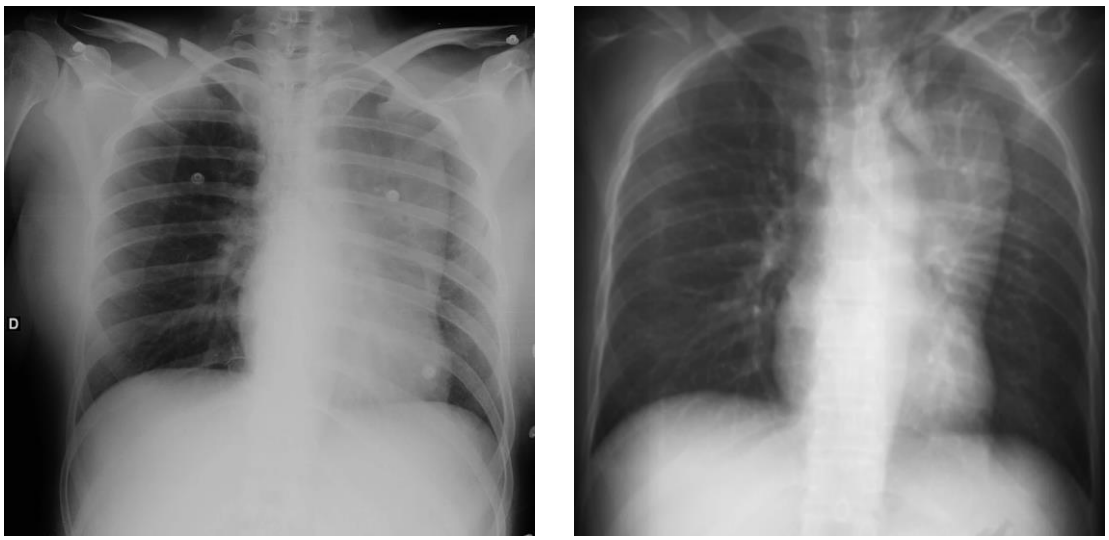

(a) **(b)**

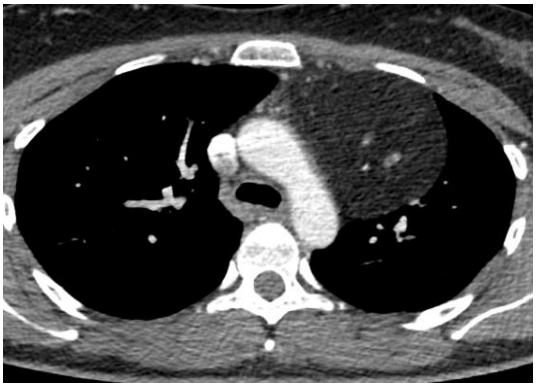

(c)

Fig. 24. Frontal chest X-ray **(a)** and coronal CT scan with MPVR reformatting (slice thickness: 128 mm) **(b)** show obliteration of the aortic knob and the upper left cardiac silhouette, suggesting that the lesion lies in the same plane as these structures. The lesion forms obtuse angles with the adjacent lung parenchyma, supporting a mediastinal origin of the lesion. In addition, its lower attenuation compared to the mediastinum is a subtle clue suggestive of a fatty lesion. Axial CT scan in mediastinal window **(c)** confirms the presence of a large mediastinal lipoma.

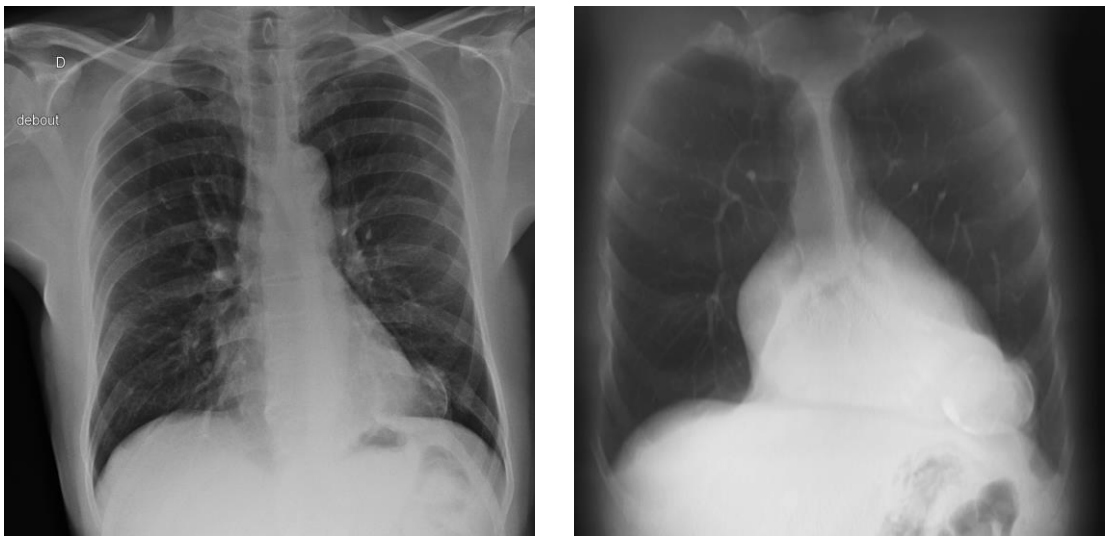

(a) **(b)**

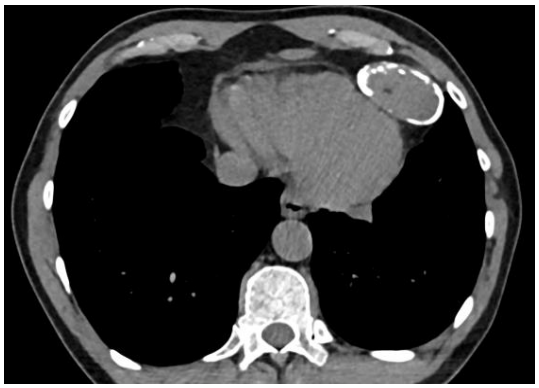

(c)

Fig. 25. Frontal chest X-ray **(a)** and coronal CT scan with MPVR reformatting (slice thickness: 256 mm) **(b)** show an oval mass with partially calcified contours, projected over the apex of the heart and the left diaphragmatic dome on both modalities. The apex of the heart appears partially obscured, whereas the diaphragmatic dome remains clearly visible. Based on the silhouette sign, this suggests a paracardiac location of the lesion. On axial CT scan in mediastinal window **(c)**, a small fatty component is visible, suggesting a paracardiac teratoma.

The silhouette sign serves as the foundation of the cervicothoracic sign, thoracoabdominal sign, and hilum overlay sign (37).

4.2. Cervicothoracic sign

The cervicothoracic sign is based on evaluating the interface between an opacity and the cervical soft tissues on a frontal chest radiograph. A positive cervicothoracic sign is observed when a lesion reaches or abuts the neck region, causing its upper margins to become indistinct on the radiograph, as they are no longer silhouetted by the surrounding aerated lung (38).

This sign helps determine whether a mediastinal mass is located anteriorly or posteriorly in relation to the trachea.

Prerequisite: understanding the anatomical boundaries of the superior mediastinum/lung apex.

- The anterior mediastinum and anterior lung apex does not extend above the clavicular level.
- The posterior mediastinum and posterior lung apex, by contrast, continues above the clavicles.

Applications of the cervicothoracic sign:

- Lesions in the anterosuperior compartment cannot project over the clavicular level and lose their upper definition at this point, indicating continuity with the cervical soft tissues (fig. 26).
- Masses in the posterosuperior compartment may project above the clavicles (39). If their upper contours remain visible, they are still outlined by air and not in contact with neck tissues (fig. 27). When the margins are no longer distinguishable, it suggests that the lesion is directly abutting the cervical soft tissues (fig. 28).
- Paratracheal lesions, being part of the middle mediastinum, may show slight extension beyond the clavicular level (40).

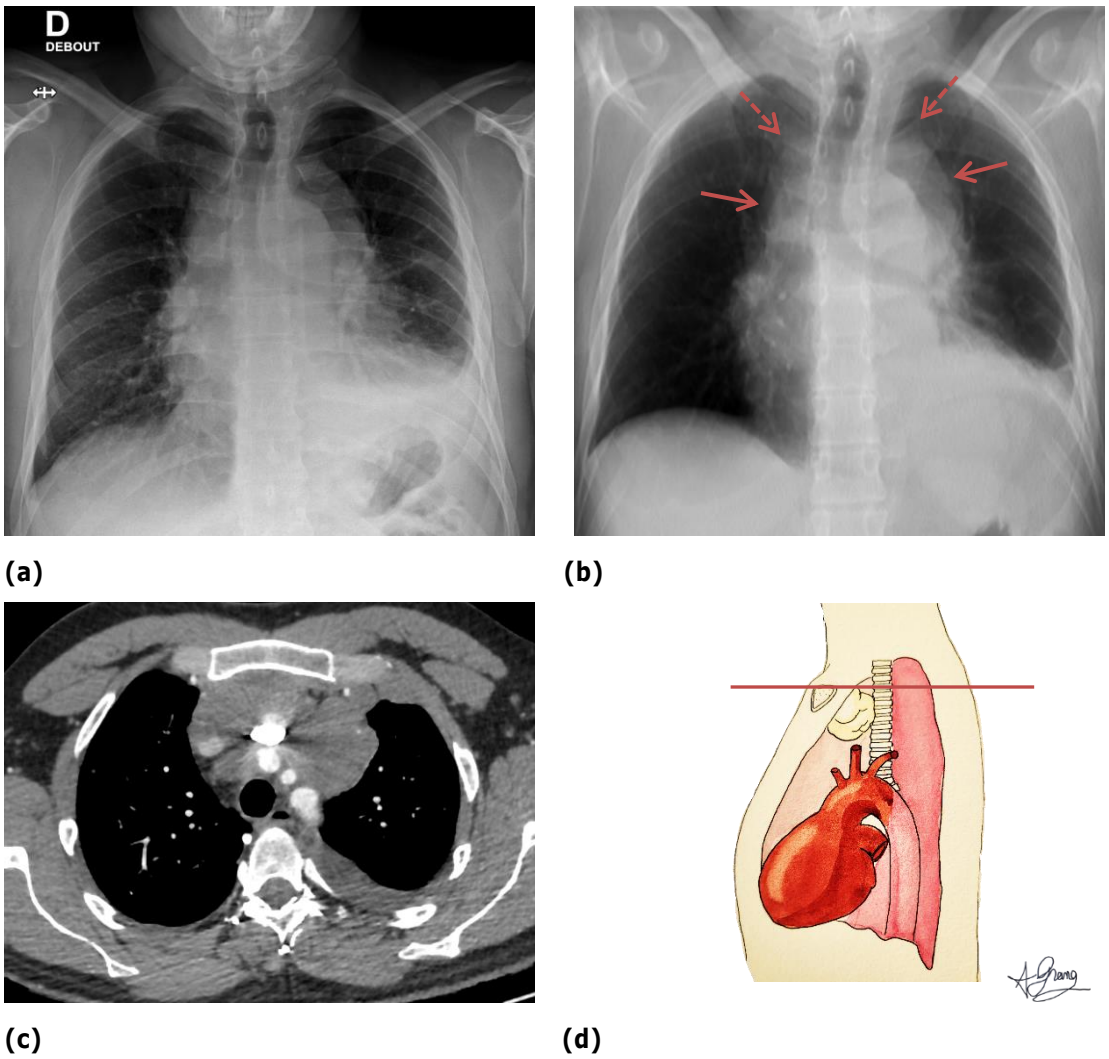

Fig. 26. Frontal chest X-ray **(a)** and coronal CT scan with MPVR reformatting (slice thickness: 200 mm) **(b)** show a widening of the superior mediastinum, with the upper margins not extending above the level of the clavicles bilaterally, suggesting an anterior mediastinal mass. The lateral borders of the mass appear well-defined below the clavicular level (solid red arrows) but gradually disappear above this level (red dashed arrows). Axial CT scan in mediastinal window **(c)** supports this suspicion, with features highly suggestive of lymphoma.
Diagram **(d)** represents a sagittal section of the thorax: the anterior mediastinum is shaded in light pink and contains an apical mass depicted in yellow; the middle mediastinum includes the heart and trachea, while the posterior mediastinum appears in dark pink. The mass lies below the red clavicular reference line and comes into contact with the cervical soft tissues, creating the positive cervicothoracic sign.

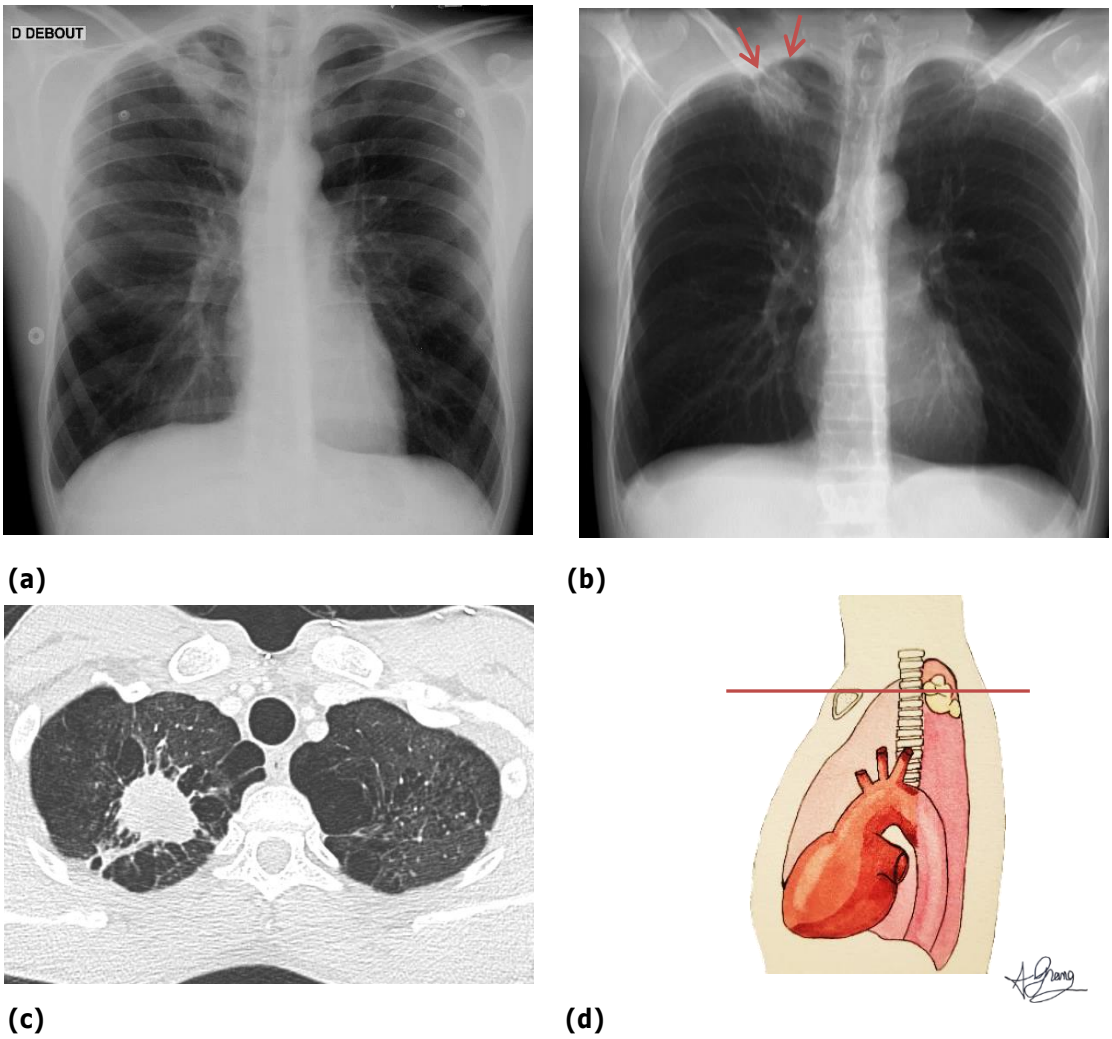

Fig. 27. Chest X-ray **(a)** and coronal CT scan with MPVR reformatting (slice thickness: 128mm) **(b)** show a mass which has an upper border extending above the clavicular level (indicating a posterior location), with a thin rim of aerated lung still visible above it (red arrows), indicating no contact with the cervical soft tissues (negative cervicothoracic sign). Axial CT scan in lung window **(c)** confirms the posterior location of the lesion relative to the trachea. This case is illustrated by diagram **(d)**.

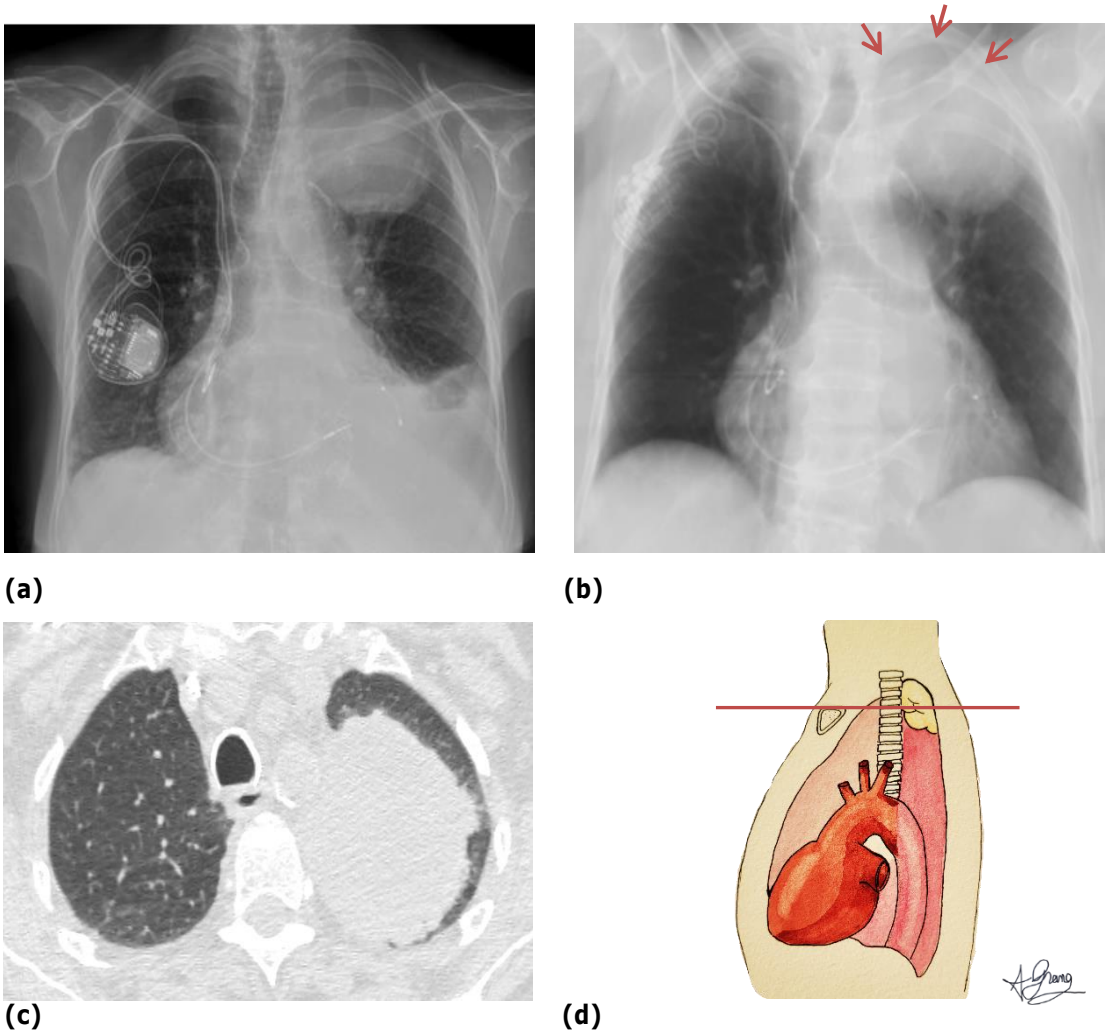

Fig. 28. Case of an apical mass extending above the level of the clavicles (red arrows) with indistinct upper borders on frontal chest X-ray **(a)** and coronal CT scan with MPVR reformatting (slice thickness: 128 mm) **(b)**. These findings suggest a posterior location and a positive cervicothoracic sign. Axial CT scan in lung window **(c)** confirms the location of the lesion.
This case is illustrated in diagram **(d)**: The posterior apical mass extends above the clavicular level and abuts the soft tissues of the neck, creating the positive cervicothoracic sign.

4.3. Thoracoabdominal sign

This sign helps localize a basal opacity. If the lower borders of the lesion are visible below the level of the diaphragmatic domes, it suggests that the lesion is purely intrathoracic, as it is remains silhouetted by air even along its lower portion (negative sign). It is therefore located in the region of the posterior costophrenic recess, which is deeper than the anterior one (fig. 29).

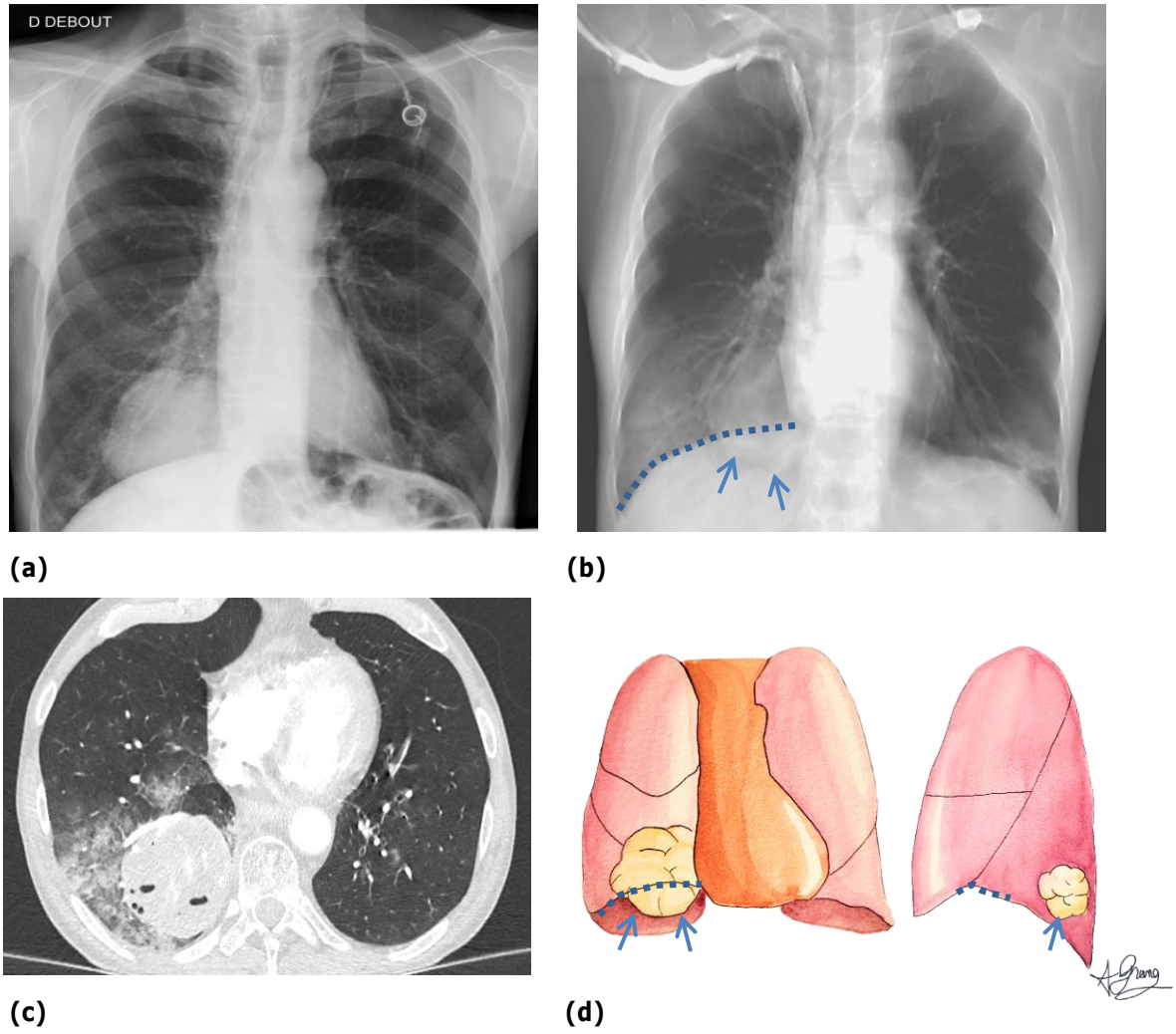

Fig. 29. Frontal chest X-ray **(a)** and coronal CT scan with MPVR reformatting (slice thickness: 128 mm) **(b)** demonstrate a right lower lobe pulmonary mass whose inferior borders (blue arrows) remain visible below the level of the diaphragmatic dome (outlined in blue dashed lines), indicating a right lower lobe origin. On axial CT scan in lung window **(c)**, areas of ground-glass opacities and peritumoral consolidations are observed, consistent with alveolar hemorrhage (CT performed a few days after the chest X-ray). Illustration **(d)** depicts the negativity of the thoracoabdominal sign.

Conversely, if the borders of the opacity disappear at the level of the diaphragmatic dome, this indicates that it is not bordered by aerated lung below this level, indicating that the lesion extends both intrathoracically and intra-abdominally (positive sign). This is known as the 'iceberg sign,' as only the visible portion of the lesion is seen, much like the tip of an iceberg (fig. 30).

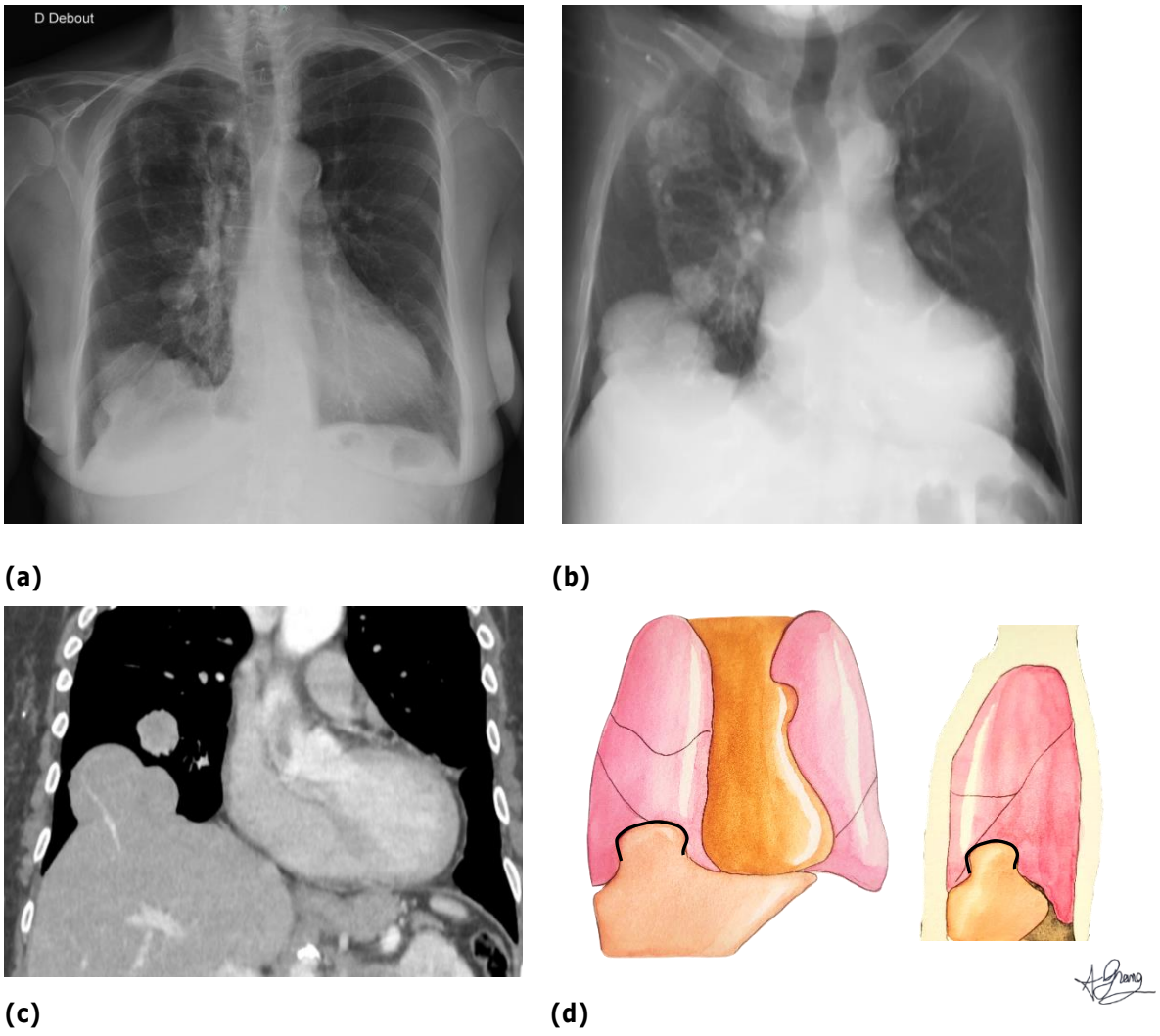

Fig. 30. Frontal chest X-ray **(a)** and coronal CT scan with MPVR reformatting (slice thickness: 128 mm) **(b)** show a polylobulated, pseudonodular opacity located in the region of the right lung base. Its lower margins are not visualized below the level of the diaphragmatic dome, suggesting a lesion with both thoracic and abdominal components ("iceberg sign"). On coronal CT scan in mediastinal window **(c)**, the diagnosis is consistent with an intrathoracic hepatic hernia. Diagram **(d)** depicts this hernia in a coronal and a sagittal view, lacking an air interface, which prevents inferior border delineation.
Additionally, on the CXR, a purely intrathoracic nodule is noted near the right pulmonary hilum. The opacity projected over the right upper lobe, with a "cuttlefish bone" appearance, corresponds to a calcified pleural plaque.

For basal opacities in the paravertebral position, the rule is slightly different. If a lesion's lower edge gradually converges towards the spine, it is likely of purely intrathoracic origin (negative sign) (fig. 31-32).

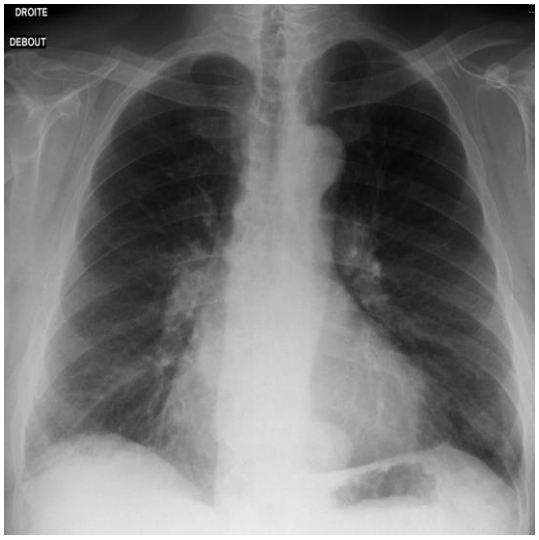

(a)

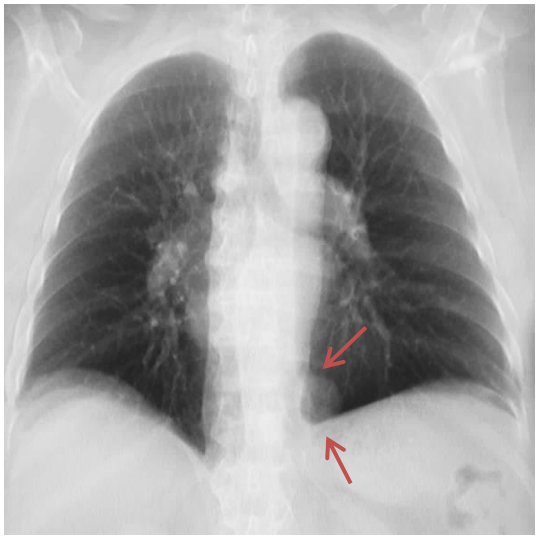

(b)

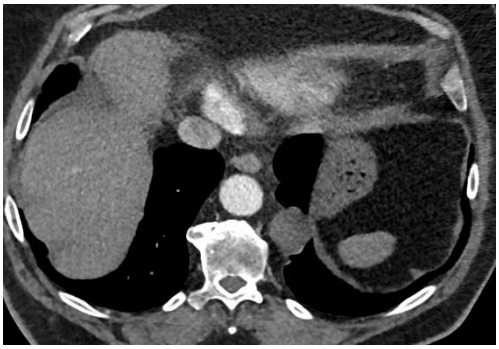

(c)

Fig. 31. On frontal chest X-ray **(a)** and coronal CT scan with MPVR reformatting (slice thickness: 128 mm) **(b)**, an ovoid lesion (red arrows) is seen in the left lower paramediastinal region, causing deviation of the paravertebral line. The inferior margin of the lesion converges towards the spine, indicating that it is of purely intra-thoracic origin. On axial CT scan in mediastinal window **(c)**, this lesion appears to have fluid attenuation.

Conversely, if the lower margin diverges, or at least does not converge towards the spine, then this formation probably has an intra-abdominal component in addition to its thoracic portion (positive sign) (fig. 32).

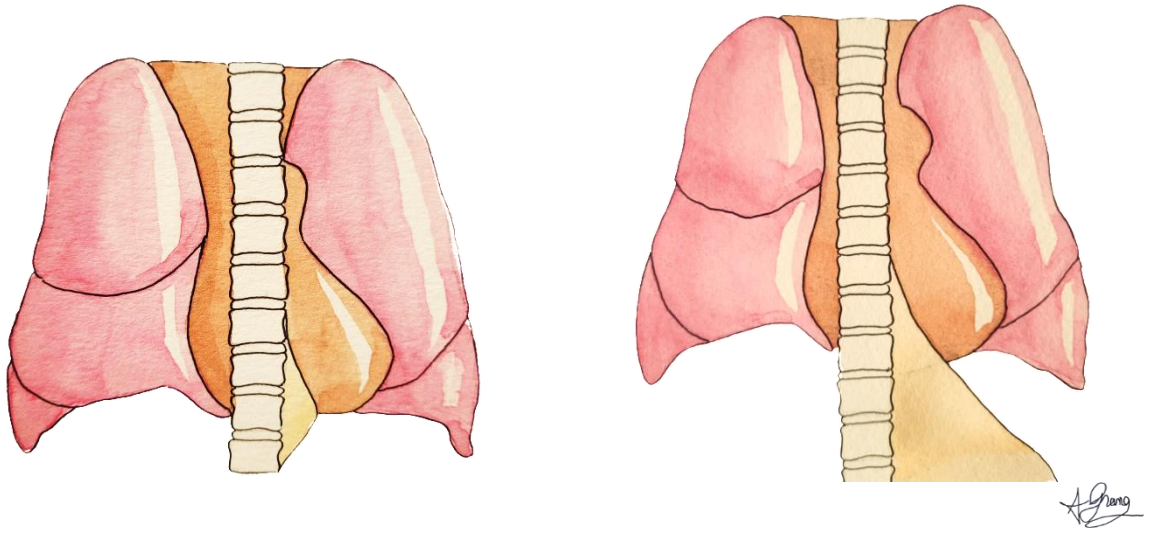

(a) **(b)**

Fig. 32. Illustration **(a)** shows a strictly intrathoracic mass with its lower border converging towards the spine below the level of the diaphragmatic dome. In contrast, illustration **(b)** depicts a lesion whose lower border gradually diverges from the spine, indicating both thoracic and abdominal components.

4.4. Hilum overlay sign – Hilum convergence sign

In the case of an opacity projected over the hilar region, if the outlines of the pulmonary vessels remain visible through the opacity, this indicates that the opacity is located either anterior or posterior to the hilum, but does not originate from it, corresponding to the hilum overlay sign (41). Moreover, if the mass obscures the cardiac border, it can be assumed to be located anterior to the hilum. Conversely, if the cardiac silhouette is preserved, the mass is likely posterior to the hilum (fig. 33).

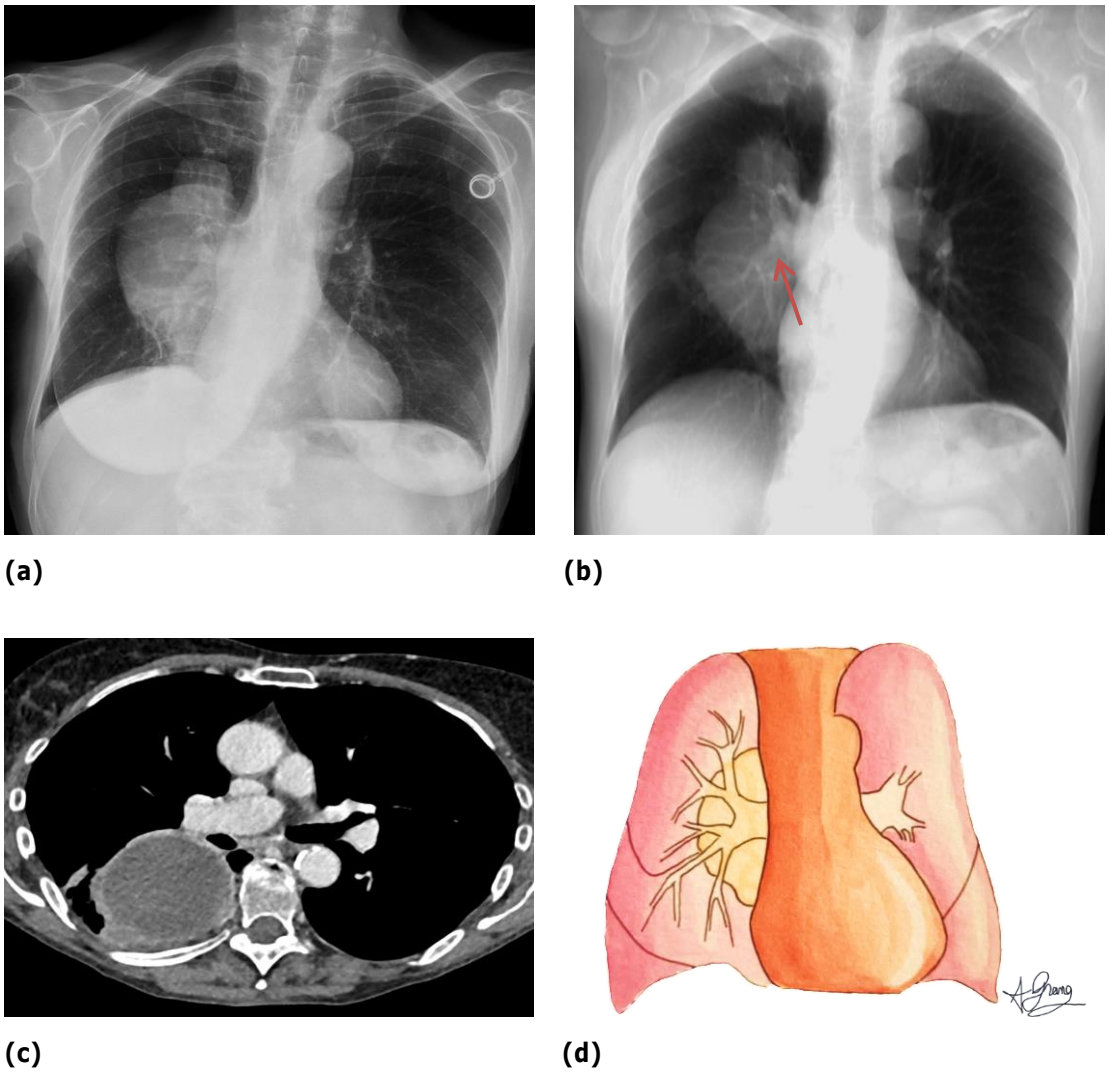

Fig. 33. Frontal chest X-ray **(a)** and coronal CT scan with MPVR reformatting (slice thickness: 128 mm) **(b)** depict a right perihilar mass. The visualization of vessels projecting through the mass (red arrow) indicates it does not originate from the hilum. Furthermore, the preservation of the right atrium silhouette confirms that the mass is located in a retrohilar position, as confirmed by axial CT scan in mediastinal window **(c)**. This sign is illustrated in diagram **(d)**. This mass corresponds to a bronchial adenocarcinoma.

On the other hand, if an opacity arises from the pulmonary hilum itself, the outlines of the pulmonary vessels will be obscured in that area, as they are no longer silhouetted by the adjacent aerated lung (absence of the hilum overlay sign). If the pulmonary vessels converge toward the opacity and become obscured along its outer margin, the lesion is most likely vascular in origin, as seen in cases of pulmonary artery enlargement due to pulmonary hypertension (fig. 34). This radiographic appearance corresponds to the hilum convergence sign (41).

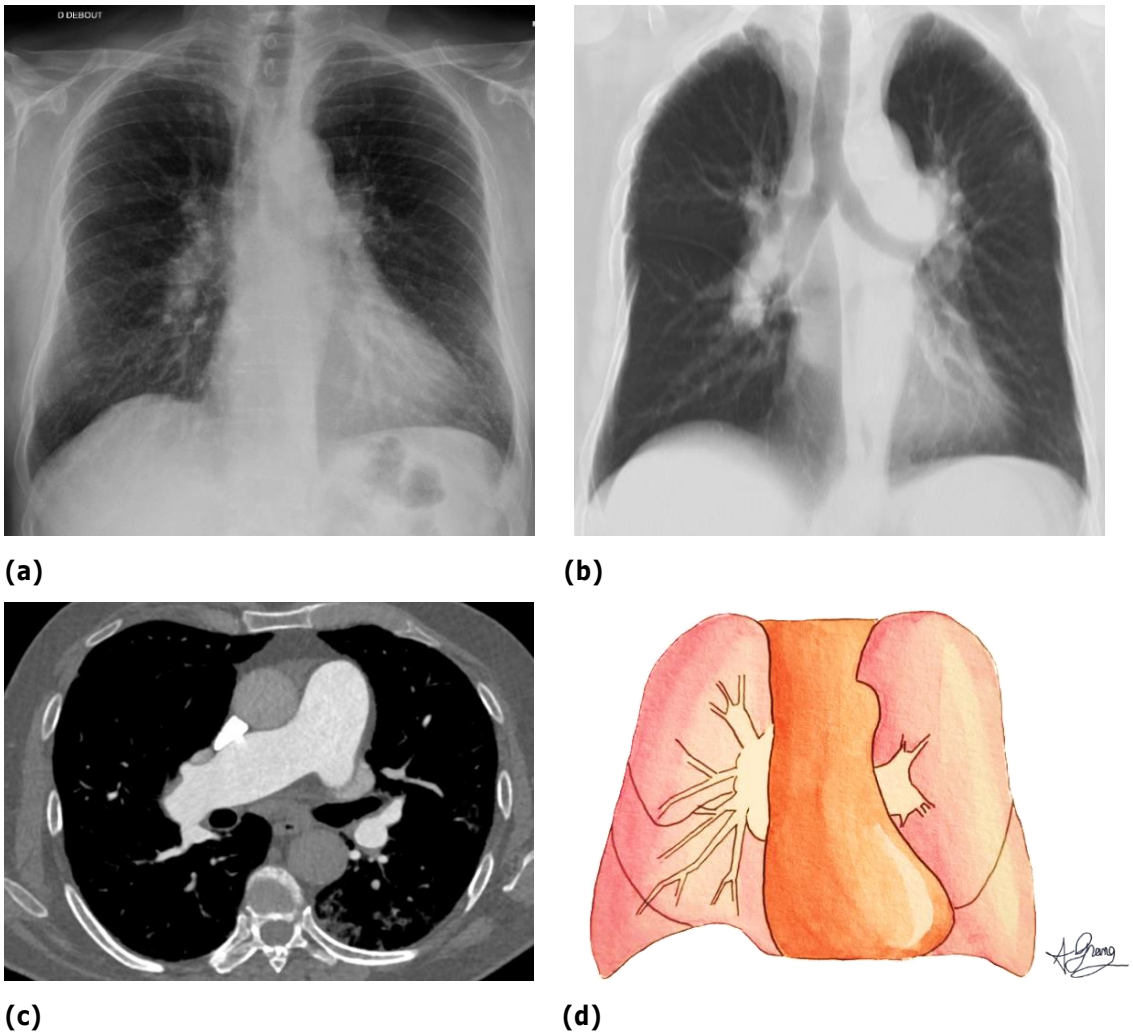

Fig. 34. On frontal chest X-ray **(a)** and coronal CT scan with MPVR reformatting (slice thickness: 64 mm) **(b)**, perihilar opacities are observed. The absence of visible vascular structures within these opacities suggests that they originate from the hilum itself. Pulmonary vessels converge normally toward the hilum, without evidence of displacement. These findings are consistent with dilated pulmonary arteries in the context of pulmonary hypertension, better appreciated on axial CT scan in mediastinal window **(c)**. This sign, known as the "hilum convergence sign" is illustrated in drawing **(d)**.

4.5. Extrapleural sign

This sign refers to the fact that opacity of extraparenchymal origin (pleural, parietal, nerogenic, etc.) forms progressive obtuse angles with the thoracic wall. On a frontal chest X-ray, an extrapulmonary lesion on the lateral chest wall typically appears with a well-defined inner edge, as its border is tangent to the X-ray beam, giving a so-called "teardrop" appearance (fig. 35).

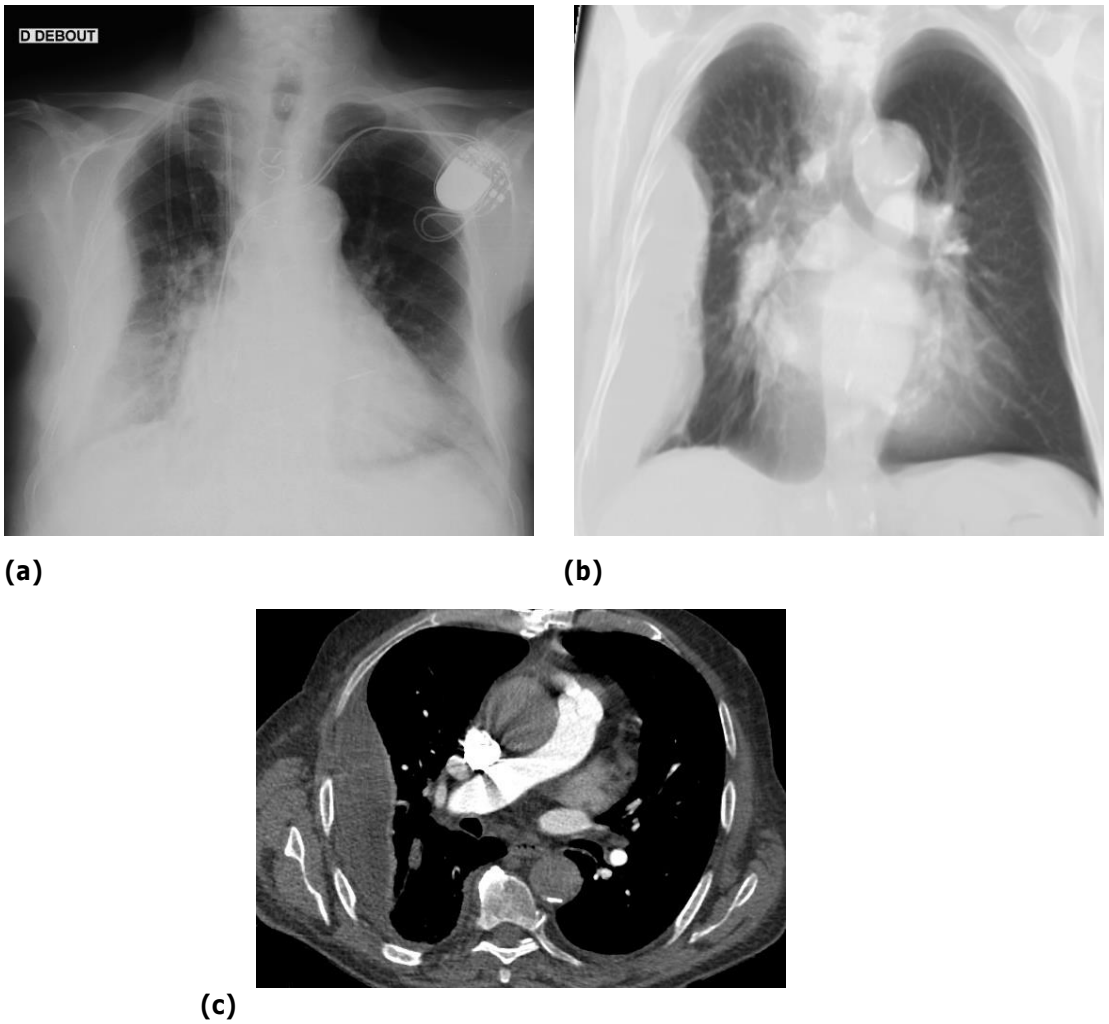

(a) **(b)**

(c)

Fig. 35. Frontal chest X-ray **(a)** and coronal CT scan with MPVR reformatting (slice thickness: 64 mm) **(b)** reveal a loculated pleural effusion adjacent to the right lateral thoracic wall, producing the characteristic "teardrop" appearance. The obtuse angles formed between the lesion and the thoracic wall suggest an extraparenchymal origin. This finding is confirmed on axial CT scan in mediastinal window **(c)**.

This stands in contrast to an intrapulmonary nodule where an acute angle would be expected where it interfaces with the lung periphery (fig. 36).

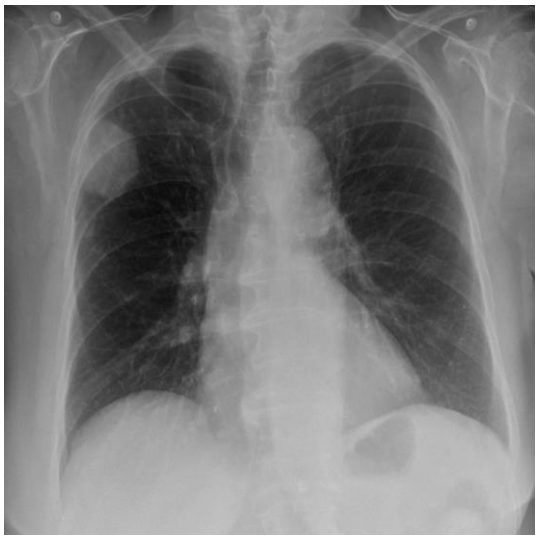

(a)

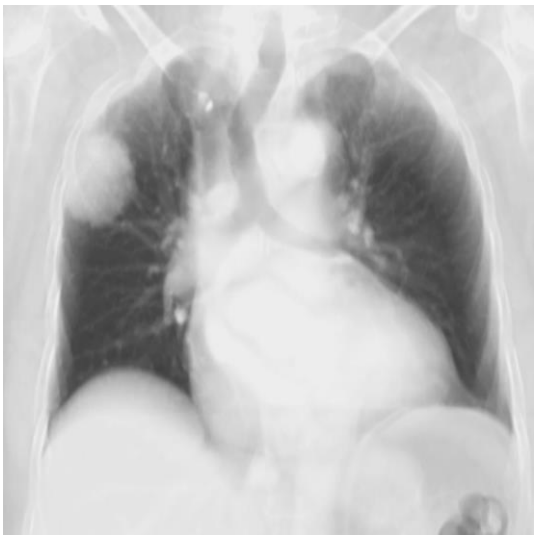

(b)

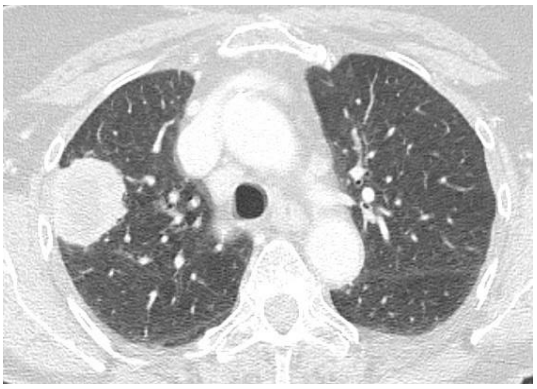

(c)

Fig. 36. On frontal chest X-ray **(a)** and coronal CT scan with MPVR reformatting (slice thickness: 64 mm) **(b)**, and axial CT scan in mediastinal window **(c)**, a pulmonary nodule adjacent to the pleura is observed. The acute angles between the nodule and the thoracic wall (Bernou's angle) indicate an intrapulmonary origin.

By extrapolation, the extrapleural sign can also be applied to paramediastinal lesions to determine whether their origin is mediastinal or intrapulmonary (fig. 37).

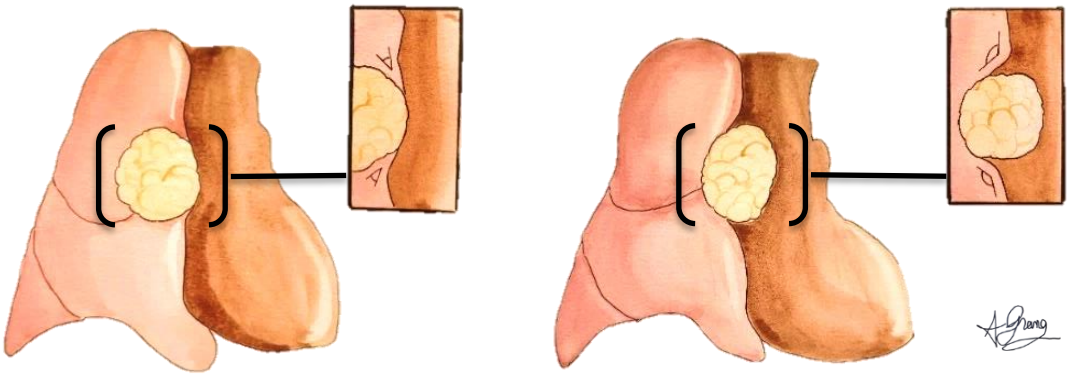

(a) **(b)**

Fig. 37. In diagram **(a)**, the angles between the lesion and the mediastinum are acute, supporting a parenchymal origin. In contrast, in diagram **(b)**, the angles are obtuse, indicating a mediastinal origin of the mass.

However, if a lesion of extrapulmonary origin is located strictly anteriorly or posteriorly in the ribcage, its margins will appear non-tangential to the X-ray beam and thus poorly defined (fig. 38).

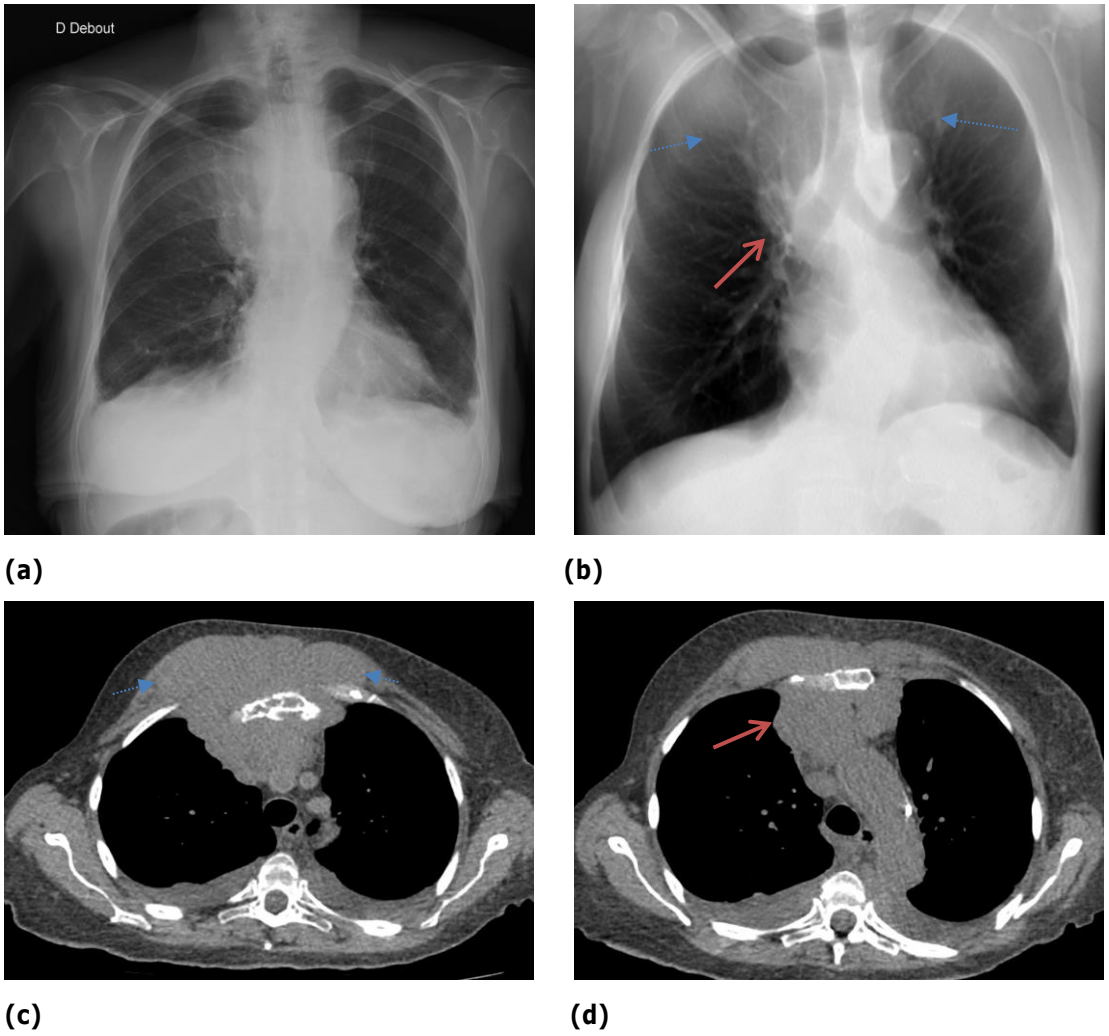

Fig. 38. Frontal chest X-ray **(a)** and coronal CT scan with MPVR reformatting (slice thickness: 128 mm) **(b)** show a poorly defined opacity projected over the upper paramediastinal region, with indistinct and blurred borders (blue dashed arrow), suggesting an extrapulmonary, likely chest wall origin. Notably, some portions—especially the inferior margin—appear better delineated (red arrow), raising suspicion of mediastinal infiltration. Additionally, the opacity does not extend above the level of the clavicles, supporting its anterior location.
Axial CT images in mediastinal window **(c)** and (**d)** confirmed the presence of a parietal lesion consistent with a plasmacytoma arising from the sternum with anterior mediastinal extension. The image (d), taken a few slices below (c), shows the mediastinal infiltration. At this level, the lateral margins of the infiltration are tangential to the X-ray beam, which explains the sharply defined inferior borders of the lesion on the radiograph.

4.6. Incomplete border sign

Incomplete border sign (fig. 39) is used to characterize an extrapulmonary opacity located anterolaterally or posterolaterally in the rib cage on CXR. This sign is also based on whether the margins of a lesion are tangential to the X-ray beam or not. In this location, an extrapulmonary lesion typically presents a well-defined inner margin and an ill-defined outer margin (42-44). The inner border appears sharp because it lies tangential to the X-ray beam, creating high contrast with the adjacent pulmonary parenchyma. By comparison, the outer margin is not tangential to the beam and merges with the pleura or chest wall, making it indistinct.

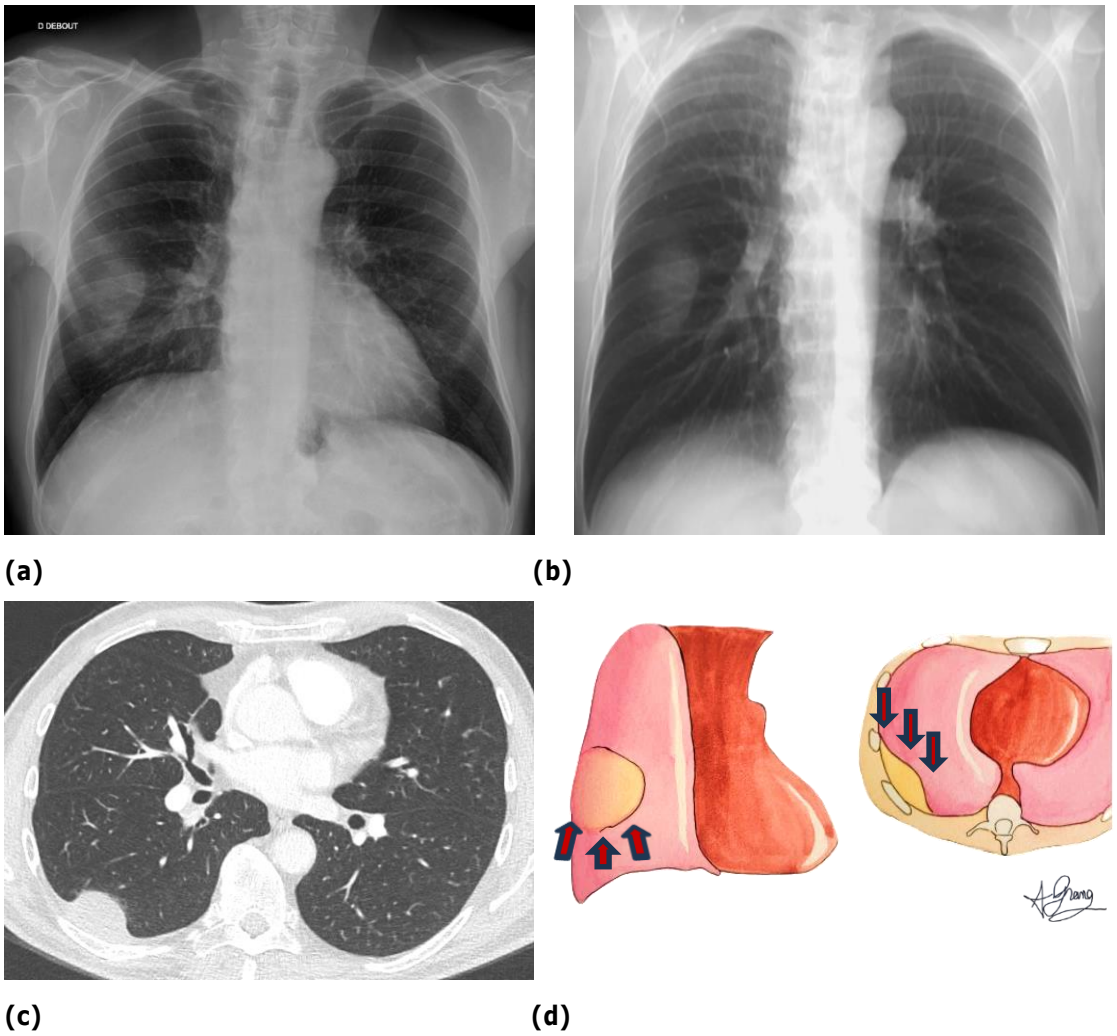

Fig. 39. Frontal chest X-ray **(a)** and coronal CT scan with MPVR reformatting (slice thickness: 64 mm) **(b)** expose a pleural metastasis. The inner border of the lesion appears well-defined due to its tangency to the X-ray beam, whereas the outer margin appears blurred because the X-ray beam is not aligned tangentially with it. This phenomenon is further illustrated on axial CT scan in parenchymal window **(c)** and in accompanying diagram **(d)**.

4.7. Air bronchogram

An air bronchogram (fig. 40) refers to the presence of air-filled bronchi or bronchioles coursing through an area of alveolar consolidation. This sign supports the intrapulmonary origin of a lesion but does not provide any indication regarding its benign or malignant nature.

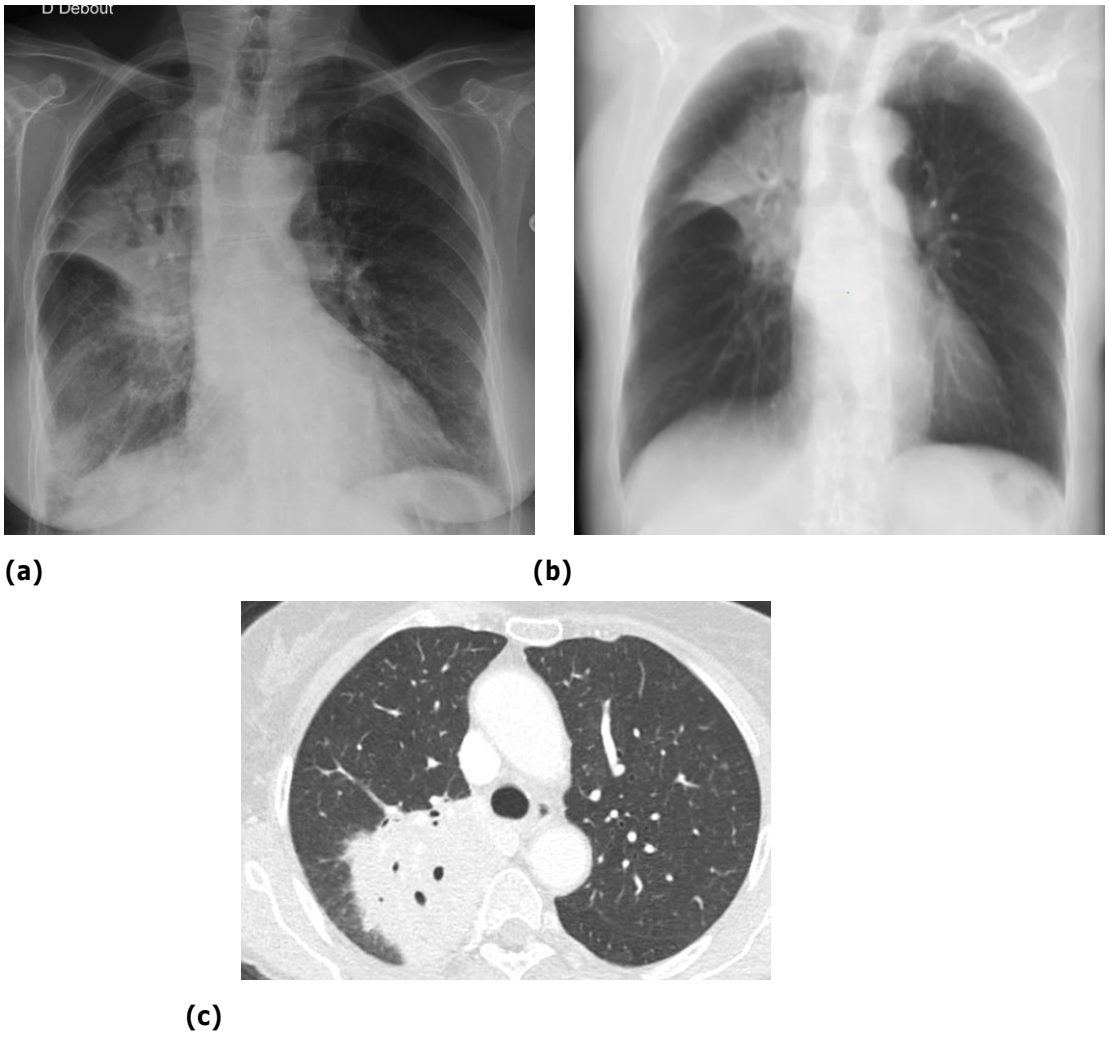

(a) **(b)**

(c)

Fig. 40. Case of a right upper lobe apical consolidation with a systematic appearance, outlining air-filled bronchi and bronchioles, creating a characteristic air bronchogram. This sign is clearly visible on frontal chest X-ray **(a)**, coronal CT scan with MPVR reconstruction (slice thickness: 128mm) **(b),** and corresponding axial CT scan in parenchymal window **(c)**. This consolidation was confirmed histologically as pulmonary lymphoma.

CONCLUSION

Despite the widespread availability of multi-detector CT, chest X-ray remains a commonly prescribed imaging exam. However, it is still prone to frequent interpretation errors. Being aware of the most commonly missed findings and understanding the underlying causes of CXR misinterpretation are key to developing practical strategies to reduce diagnostic errors. Ultimately, the challenge of CXR lies not in what it shows, but in what it hides.

REFERENCES

(1) Calli E, Sogancioglu E, van Ginneken B, van Leeuwen KG, Murphy K. Deep learning for chest X-ray analysis: a survey. Medical Image Analysis. 2021;72:102125.

(2) Donald JJ, Barnard SA. Common pattern in 558 diagnostic radiology errors. J Med Imaging Radiat Oncol. 2012;56(2):173-178.

(3) Gefter WB, Post BA, Hatabu H. Commonly Missed Findings on Chest Radiographs: Causes and Consequences. Chest. 2023 Mar;163(3):650-661.

(4) Waite S, Scott J, Gale B, et al. Interpretive error in radiology. AJR Am J Roentgenol. 2017;208(4):1-11.

(5) Bruno MA, Walker EA, Abujudeh HH. Understanding and confronting our mistakes: the epidemiology of error in radiology and strategies for error reduction. Radio Graphics. 2015;35(6):1668-1676.

(6) Garland LH. On the scientific evaluation of diagnostic procedures. Radiology. 1949;52(3):309-328.

(7) Berlin L. Radiologic errors and malpractice: a blurry distinction. AJR Am J Roentgenol. 2007;189(3):517-522.

(8) Berlin L. Accuracy of diagnostic procedures: has it improved over the past five decades? AJR Am J Roentgenol. 2007;188(5):1173-1178.

(9) Kundel HL, Nodine CF, Carmody D. Visual scanning, pattern recognition and decision-making in pulmonary nodule detection. Invest Radiol. 1978;13(3):175-181.

(10) Gibbs JM, Chandrasekhar CA, Ferguson EC, Oldham SAA. Lines and stripes: where did they go? From conventional radiography to CT. RadioGraphics 2007;27(1):33–48.

(11) Jhala K, Madan R, Hammer M. A pictorial review of lung torsion using 3D CT cinematic rendering. Emerg Radiol 2021;28(1):171–176.

(12) Takahashi K, Sugimoto H, Ohsawa T. Obliteration of the descending aortic interface in pectus excavatum: correlation with clockwise rotation of the heart. Radiology 1992;182 (3): 825-8.

(13) Hapuarachchi K, Cowan I. The medial breast margin sign: A new sign of pectus excavatum in adult females and comparison with classic signs. Journal of Medical Imaging and Radiation Oncology 2019;63 (6):737-44.

(14) de Pádua Gomes de Farias LPG, Menezes DC, Faé IS, de Arruda PHC, Santos JMMM, Teles GBDS. Anatomical variations and congenital anomalies of the ribs revisited by multidetector computed tomography. Radiol Bras. 2020 Nov-Dec;53(6):413-418.

(15) Nair R, Muthukuru SR. Dextrocardia. In: StatPearls [Internet]. Treasure Island (FL): StatPearls Publishing; 2022 [cited 2025 Jun 27].

(16) Cinà CS, Althani H, Pasenau J, Abouzahr L. Kommerell's diverticulum and right-sided aortic arch: a cohort study and review of the literature. Journal of vascular surgery 2004;39 (1):131-9.

(17) Zhu Y-Q, Li M-H, Fang C, Wang W, Tan H-Q, Cheng Y-S. Combined endovascular and vascular surgical therapy of a blister-like distal internal carotid aneurysm in a patient with a right-sided aortic arch. Vascular 2010;18(6):363–366.

(18) Noguchi K, Hori D, Nomura Y et-al. Double aortic arch in an adult. Interact Cardiovasc Thorac Surg. 2012;14 (6): 900-2.

(19) Hanneman K, Newman B, Chan F. Congenital Variants and Anomalies of the Aortic Arch. RadioGraphics 2017;37(1):32–51.

(20) Albay S, Cankal F, Kocabiyik N, Yalcin B, Ozan H. Double Superior Vena Cava. Morphologie. 2006;90(288):39-42.

(21) Demos TC, Posniak HV, Pierce KL et-al. Venous anomalies of the thorax. AJR Am J Roentgenol 2004;182 (5): 1139-50.

(22) Bass JE, Redwine MD, Kramer LA et-al. Spectrum of congenital anomalies of the inferior vena cava: cross-sectional imaging findings. Radiographics 2000;20 (3): 639-52.

(23) Jiao A, Nadim B, Hammer M, Jhala K. 3D Visual Guide to Lines and Stripes in Chest Radiography. Radiographics. 2023 Sep;43(9):e230017.

(24) Jariwala P, Maturu VN, Christopher J, Jadhav KP. Congenital isolated unilateral agenesis of pulmonary arteries in adults: case series and review. Indian J Thorac Cardiovasc Surg. 2021 Jan;37(Suppl 1):144-154.

(25) Woodring JH, Daniel TL. Mediastinal analysis emphasizing plain radiographs and computed tomograms. Med Radiogr Photogr 1986;62:1–48.

(26) Proto AV. Mediastinal anatomy: emphasis on conventional images with anatomic and computed tomographic correlations. J Thorac Imaging 1987; 2:1– 48.

(27) Giron J, Fajadet P, Sans N, et al. Diagnostic approaches to mediastinal masses. Eur J Radiol 1998;27:21–42.

(28) Proto AV, Simmons JD, Zylak CJ. The posterior junction anatomy. Crit Rev Diagn Imaging 1983; 20:121–173.

(29) Proto AV, Corcoran HL, Ball JB. The left paratracheal reflection. Radiology 1989;171:625–628.

(30) Keats TE. The aortic-pulmonary mediastinal stripe. Am J Roentgenol Radium Ther Nucl Med1972;116:107–109.

(31) McComb BL. Reflecting upon the left superior mediastinum. J Thorac Imaging 2001;16:56-64.

(32) Kamenskiy A, Miserlis D, Adamson P, et al. Patient demographics and cardiovascular risk factors differentially influence geometric remodeling of the aorta compared with the peripheral arteries. Surgery 2015;158(6):1617–1627.

(33) Chasen MH. Practical applications of mach band theory in thoracic analysis. Radiology 2001;219:596–610.

(34) Jha RK, Gupta MK, Pant AR, Pandey NK. Measurement of the sub-carinal angle on the normal chest radiograph of adult at BPKIHS, Dharan, Nepal. J BP Koirala Inst Health Sci. 2019;2(2):46–51.

(35) Del Ciello A, Franchi P, Contegiacomo A, et al. Missed lung cancer: when, where and why?Diagn Interv Radiol. 2017;23(2):118-126.

(36) Felson B, Felson H. Localization of intrathoracic lesions by means of the postero-anterior roentgenogram; the silhouette sign. Radiology 1950;55 (3): 363-74.

(37) Marshall GB, Farnquist BA, MacGregor JH et-al. Signs in thoracic imaging. J Thorac Imaging 2006;21 (1): 76-90.

(38) Felson B. More chest roentgen signs and how to teach them. Annual Oration in memory of L.Henry Garland, M.D., 1903-1966. Radiology 1968;90 (3): 429-41. (cervico-tho)

(39) George PP, Irodi A, Nidugala Keshava S, Lamont AC. 'Felson Signs' revisited. *J Med Imaging Radiat Oncol*. 2014 Feb;58(1):64–74. (2ème cervicotho)

(40) Felson B. More chest roentgen signs and how to teach them. Annual Oration in memory of L.Henry Garland, M.D., 1903-1966. Radiology 1968;90 (3): 429-41.

(41) Gaeta M, Volta S. Hilum overlay sign and the hilum convergence sign. Eurorad [Internet]. 2006 Jun [cited 2025 Jul 19];Case 3148.

(42) Catalano O. The incomplete border sign. Radiology 2002;225 (1): 129-30.

(43) Ellis R. Incomplete border sign of extrapleural masses. JAMA 1977;237 (25): 2748.

(44) Hsu CC, Henry TS, Chung JH et-al. The incomplete border sign. J Thorac Imaging. 2014;29(4): W48.

LIST OF FIGURES

TABLE OF CONTENTS

GRANGEREAU Aurore

Interprétation rétrograde de radiographies thoraciques en reproduisant les signes radiologiques à partir d'images CT grâce à la technique de « rendu volumique direct ».

RÉSUMÉ

Introduction
La radiographie standard du thorax reste un outil fondamental en imagerie thoracique. Cependant, sa bonne interprétation n'est pas toujours évidente et nécessite une compréhension approfondie des signes radiologiques responsables des aspects radiographiques observés.
Objectifs
- Mettre en évidence et identifier les signes sémiologiques sur la radiographie thoracique à travers des reconstructions MPVR (Multiplanar Volume Rendering) d'images scanner.
- Apprendre à reconstruire rétrospectivement l'aspect macroscopique des lésions thoraciques sur la radiographie thoracique en se basant sur des signes radiologiques de plus en plus souvent négligés.
Messages à retenir
Il existe quatre grandes catégories de régions anatomiques ou de structures susceptibles d'être mal interprétées sur la radiographie thoracique :
1. Variantes anatomiques des structures médiastinales et illusions radiologiques (anomalies congénitales sans expression clinique comme la proéminence de l'arc azygos, l'arc aortique droit, les kystes bronchogéniques et pleuro-péricardiques…).
2. Perception des lésions médiastinales : Le médiastin contient de multiples interfaces anatomiques orientées selon différents plans, ce qui rend l'interprétation de leurs limites difficile. Une interprétation fiable nécessite de comprendre comment les structures anatomiques médiastinales se projettent sur la radiographie thoracique, produisant des signes caractéristiques d'interface bidimensionnelle.
3. Zones aveugles ou cachées : Certaines zones sont des pièges dans l'interprétation des radiographies thoraciques à cause d'une opacité accrue liée à des structures anatomiques normales. Celles-ci incluent les apex pulmonaires, les régions hilaires, la zone rétrocardiaque, et les régions rétro-diaphragmatiques.
4. Localisation des opacités thoraciques : Plusieurs signes aident à déterminer la localisation exacte d'une opacité thoracique et à confirmer ou non son origine pulmonaire. Parmi eux : le signe de la silhouette, le signe cervicothoracique, le signe thoraco-abdominal, etc.

Mots-clés : Radiographie thoracique, MPVR, lignes médiastinales, variantes anatomiques médiastinales, zones pièges

Retrograde interpretation of chest X-rays by reproducing radiological signs from CT images using the "direct volume rendering" technique

ABSTRACT

Introduction
The standard chest X-ray remains the foundational tool in thoracic imaging. However, its proper interpretation is not always straightforward and requires a thorough understanding of the radiologic signs responsible for the observed radiographic appearances.
Objectives
- To highlight and identify semiological signs on chest X-ray through MPVR (Multiplanar Volume Rendering) reconstructions from CT images.
- To learn how to retrospectively reconstruct the macroscopic appearance of thoracic lesions on chest X-ray.
Take-Home Message
There are four main categories of anatomical regions or structures that are prone to misinterpretation on chest radiography:
1. Anatomical Variants of the mediastinal structures and radiological illusions (congenital anomalies with no clinical expression like azygos arch prominence, right-sided aortic arch, bronchogenic and pleuropericardial cysts)
2. Perception of mediastinal lesions: The mediastinum contains multiple anatomical interfaces oriented in different planes, making their boundaries challenging to interpret. Reliable interpretation requires an understanding of how mediastinal anatomical structures reflect onto the chest X-ray, producing characteristic two-dimensional interface signs.
3. Blind spots or hidden areas: There are pitfall zones in chest X-ray interpretation due to increased opacity related to normal anatomical structures. These include the lung apices, hilar regions, retrocardiac area, and the regions beneath the diaphragmatic domes.
4. Localization of Thoracic Opacities: Several signs help determine the exact location of a thoracic opacity and confirm its pulmonary origin. These include the silhouette sign, cervicothoracic sign, thoracoabdominal sign, etc.

Keywords : Chest X-Ray, MPVR, mediastinal lines, mediastinal anatomical variants, hidden areas

FACULTÉ DE SANTÉ
UNIVERSITÉ D'ANGERS

FACULTÉ
DE SANTÉ
UNIVERSITÉ D'ANGERS